Received: 14 March 2024 | Revised: 31 May 2024 | Accepted: 6 June 2024

DOI: 10.1002/ardp.202400191

FULL PAPER

ARCH PHARM DPhG
Archiv der Pharmazie

New biologically active sulfonamides as potential drugs for Alzheimer's disease

Marie Nevyhoštěná | Alena Komersová | Vladimír Pejchal | Šárka Štěpánková | Petr Česla | Kevin Matzick | Jana Macháčková | Roman Svoboda

Faculty of Chemical Technology, University of Pardubice, Pardubice, Czech Republic

Correspondence
Marie Nevyhoštěná, Faculty of Chemical Technology, University of Pardubice, Studentská 573, 532 10 Pardubice, Czech Republic.
Email: st54183@upce.cz

Funding information
Univerzita Pardubice; Internal Grant Agency of the University of Pardubice

Abstract

A family of new compounds with sulfonamide and amide functional groups as potential Alzheimer's disease drugs were prepared by multistep synthesis. Thermal stability measurements recorded the initial decomposition in the range of 200–220°C, close above the melting point. The final compounds were tested for their ability to inhibit acetylcholinesterase and butyrylcholinesterase, and the in vitro dissolution behavior of selected compounds was studied through both lipophilic and hydrophilic matrix tablets. All nine tested derivatives were even more active in inhibiting acetylcholinesterase than the clinically used rivastigmine. Regression analysis of the obtained dissolution profiles was performed, and the effects of the pH and the release mechanism were determined. Some substances showed remarkable biological activity and became a subject of interest for further extensive study.

KEYWORDS
Alzheimer's disease, cholinesterase inhibitors, dissolution testing, sulfonamides, synthesis

1 | INTRODUCTION

A report from the World Health Organization (WHO) indicates that approximately one billion people worldwide are impacted by neurological disorders. These disorders affect individuals in every country, regardless of age, gender, education, or income levels.[1] Alzheimer's disease (AD), a neurodegenerative disorder, is marked by cognitive impairment and dementia. Current estimates suggest that around 50 million people are living with the disease.[2] As AD cases continue to increase, the burden on families, caregivers, healthcare systems, and society will intensify unless an effective treatment is discovered.[2]

From a neuropathological perspective, AD involves the loss of brain tissue due to the mass death of nerve cells, primarily in the frontal lobe and limbic system.[3] The disorder is also associated with a gradual decline in cholinergic signaling, crucial for cognitive function. Consequently, initial treatment strategies focus on symptom management through cholinesterase inhibitors to enhance acetylcholine levels. Currently, only three cholinergic drugs—donepezil, galantamine, and rivastigmine (RIV)—and an N-methyl-D-aspartate (NMDA) receptor antagonist, memantine, are available for AD treatment.[4,5] However, these medications can cause various side effects such as nausea, gastrointestinal issues, diarrhea, muscle weakness, fainting, and weight loss. Additionally, cholinergic drugs typically provide symptom relief for a limited period of up to 3 years.[6] By inhibiting the hydrolysis of acetylcholine through acetylcholinesterase (AChE)

Abbreviations: AChE, acetylcholinesterase; AD, Alzheimer's disease; API, active pharmaceutical ingredient; ATCh, acetylthiocholine; BChE, butyrylcholinesterase; BTCh, butyrylthiocholine; DTNB, 5,5'-dithiobis-2-nitrobenzoic acid; PBS, phosphate-buffered saline; RIV, rivastigmine; TGA, thermogravimetric.

and butyrylcholinesterase (BChE) inhibitors, acetylcholine levels at synapses increase, aiding in the restoration of cholinergic neurotransmission and cognitive abilities.[7] BChE inhibition becomes particularly effective as the disease advances and AChE activity declines. Nonselective compounds that inhibit both cholinesterases may improve treatment efficacy.[4,8] While cholinesterase inhibitors can temporarily alleviate AD symptoms, they do not halt disease progression.[4]

AD is one of the leading causes of death, ranking fourth to fifth globally. Research advancements in the field, including progress in neuroimaging, animal models, gene studies, and biomarkers, have been significant in recent decades.[2] Although the precise molecular mechanisms of AD remain unclear, the disorder is recognized as multifactorial. Considering the numerous biological molecules and pathways involved in the onset and progression of AD, developing multifunctional agents with synergistic effects to counteract the disease's pathogenesis holds promise for future treatment strategies.[4] Antioxidants offer a good option to combat neurodegeneration and protection against AD. Also, sulfonamides feature antibacterial, anti-inflammatory, and anticancer effects; they are also antioxidants and carbonic anhydrase inhibitors, and they are used to treat AD. Therefore, the development of new and less toxic substances along with antioxidant properties is of critical importance.[7]

The matrix tablets ensure gradual absorption and then excretion of drugs. The dissolution test is a pharmacokinetic study (in vitro) that is usually part of bioequivalence studies. This test can be used to assess the quality and stability of the drug. The dissolution profile of the drug is one of the most important characteristics of the dosage form. The dissolution curve can be used to infer the type of drug release (immediate × controlled), the type of controlled release (prolonged × delayed × pulsed), or the kinetics and mechanism of drug release. Quantitative analysis of dissolution data based on the mathematical description of the drug dissolution profile allows one to determine the mechanism of drug release and obtain kinetic parameters of drug release under in vitro conditions, which can be used to predict the mechanism and rate of drug release under in vivo conditions.[9–11]

The aim of this work was the synthesis, characterization, and dissolution testing of a family of new multifunctional compounds with a sulfonamide and amide functional group. After thermo-analytical characterization, the ability to inhibit AChE and BChE was tested for the final compounds by Ellman's method, and in vitro dissolution behavior of selected compounds was studied through lipophilic and hydrophilic matrix tablets. Because most commonly used drugs are poorly soluble in water, the research is moving toward finding solutions to "how to increase the solubility of poorly soluble drugs". One approach is to convert the drug to one of its alternative forms—that is the reason why our final compounds were converted to hydrochlorides for the dissolution tests. Regression analysis of the obtained dissolution profiles was performed, and the effects of pH and release mechanism were studied.

2 | RESULTS AND DISCUSSION

2.1 | Chemistry

A series of novel sulfonamide derivatives were successfully synthesized, as outlined in Scheme 1. Table 1 shows the list of the substituents of the final substances. The substances **3a–i** and **8**, our starting materials, were prepared according to the known procedures[12,13] The starting substances **3a–i** were converted to chlorides using $SOCl_2$. Then, the obtained compounds **4a–i** reacted with substance **8** to give the desired compounds **9a–i**. The substances **9a–i** were converted to hydrochlorides in methanol using conc. HCl to increase solubility during dissolution tests. The overall yields of targeted sulfonamides ranged from 13% to 63%.

2.2 | Thermo-analytical characterization

The final products of the syntheses, substances **10a–i**, were first characterized by means of differential scanning calorimetry (DSC) to assess the melting points and estimate the purity of the compounds. The DSC curves obtained for the synthesized sulfonamides at 10°C·min^{-1} are shown in Figure 1, where the endothermic peaks correspond to the melting of the particular compounds. In general, narrow peaks with a sharp onset indicate the melting of pure compounds, whereas broad or complex melting peaks usually suggest the presence of impurities, crystalline polymorphs, reaction side-products, or remaining reactants. In accordance, the synthesized compounds **10d**, **10e**, and **10h** (all of which are fluorinated compounds) can be categorized as highly pure; compounds **10a**, **10b**, **10c**, **10f**, and **10g** probably contain minor amounts of impurities; compounds **10a** and **10i** are suspect of containing either larger amount of side-products or forming polymorphic/eutectic phases. The DSC-determined temperatures of melting T_m (evaluated as extrapolated onsets) and the estimated melting enthalpies are listed in Table 2—note that for substances **10b** and **10i**, two T_m values are listed, corresponding to the onsets of the two distinct melting peaks. No straightforward correlation occurs between the substituent molar masses and T_m or ΔH_m, which indicates a more complex intermolecular van der Waals bonding of the synthesized compounds.

In addition to the calorimetric data, thermogravimetry was employed to monitor the heating-related mass loss for compounds **10a**–**10i** (see Figure 2). As expected, based on the structural similarity of the synthesized compounds (that was also confirmed by Raman spectroscopy—see Figure 3), very similar thermal decomposition occurs for all synthesized compounds, with the onset at ~220°C (measured at 10°C·min^{-1} in N_2 atmosphere). In air, the compounds exhibit a tendency toward slight oxidation above ~130°C, as evidenced by the 0.1%—1% mass increases. Kinetics-wise, all compounds show a multistep decomposition, with only compound **10a** (R_1 = R_2 = R_3 = H) exhibiting minor deviations in the rapidity and magnitude of the first two decomposition steps. Considering the often-low activation energies of the drugs' decomposition, the

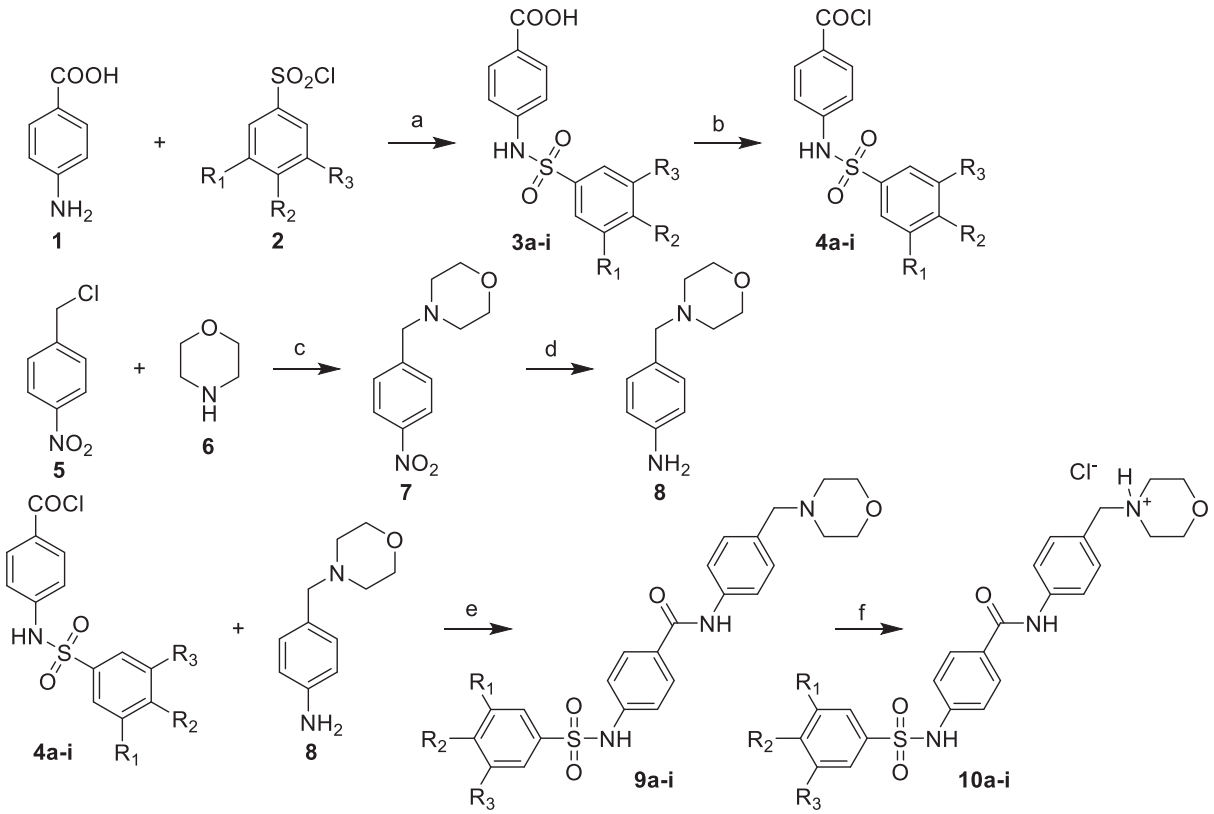

a) K_2CO_3, H_2O, 90 °C, 2 h.; b) $SOCl_2$, TOL, 90 °C, 2 h.; c) EtOH, 1 h. reflux
d) N_2H_4, $FeCl_3$, MeOH, 80 °C, 4 h.; e) K_2CO_3, DCM, 2 d.; f) HCl, MeOH

SCHEME 1 Synthesis of the novel sulfonamide derivatives **10a–i**.

TABLE 1 A list of the substituents of substances 10a–i.

	R_1	R_2	R_3
10a	H	H	H
10b	H	CH_3	H
10c	CH_3	H	CH_3
10d	F	H	F
10e	F	H	H
10f	Cl	H	Cl
10g	Cl	H	H
10h	F	CH_3	H
10i	Cl	CH_3	H

equilibrium degradation for the majority of the present compounds will most probably start close above the melting point, which will make these compounds challenging to process via hot-melt extrusion or conventional three-dimensional (3D) printing.

2.3 | In vitro evaluation of AChE- and BChE-inhibiting activity

Ellman's method[14] was used for an in vitro screening of the ability of the newly synthesized compounds to inhibit AChE from electric eel (AChE) and BChE from equine serum (BChE), and the results were compared with those for the standard RIV.[15] The inhibitory activity was expressed as IC_{50}, representing the concentration of the inhibitor causing 50% inhibition of the enzyme. To determine the IC_{50} value of a given inhibitor, it is possible to use the relationship between the ratio of the rates of uninhibited and inhibited hydrolysis and the concentration of the inhibitor.[14,16] The obtained IC_{50} values are summarized in Table 3.

In the series of nine derivatives, all were shown to be more effective in the inhibition of AChE than of BChE. Focusing on inhibition of AChE, IC_{50} values were found in a range from 7.35 µM (**10h**) to 17.13 µM (**10d**). Table 3 shows that all nine derivatives are, under the given reaction conditions, more effective in inhibiting AChE than the standard RIV. However, two derivatives (compounds **10b** and **10i**) under the given reaction conditions are more potent in inhibiting BChE than the standard RIV. The IC_{50} values were found in a range from 28.88 µM (**10i**) to >500 µM (**10d**).

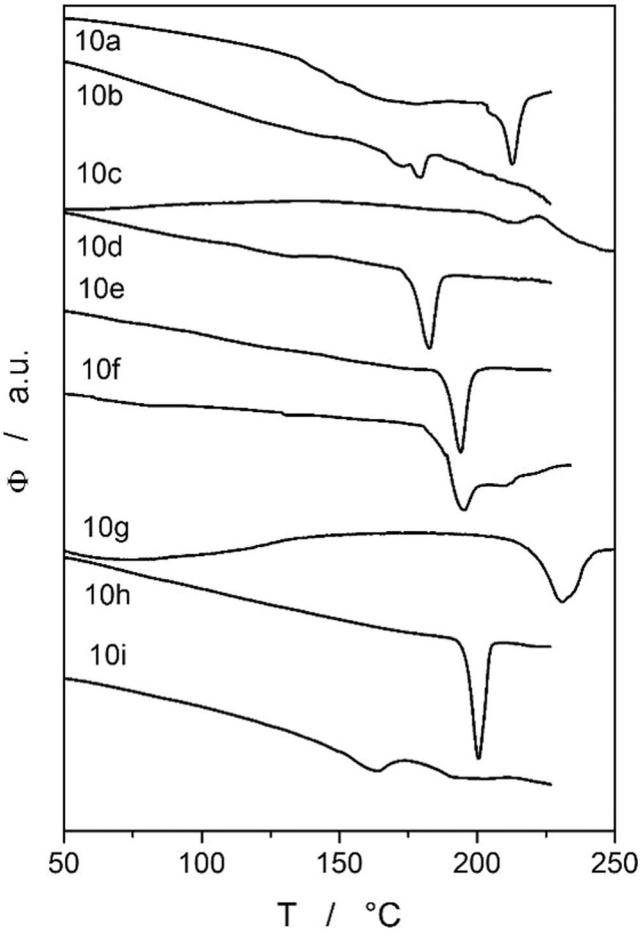

FIGURE 1 DSC curves obtained at 10°C·min^{-1} for substances **10a–i**. The exothermic effects evolve in the upward direction. DSC, differential scanning calorimetry.

TABLE 2 Melting temperatures T_m and melting enthalpies ΔH_m for substances 10a–i.

	T_m (°C)	ΔH_m (J·g^{-1})
10a	208.1	88.2
10b	164.2 & 173.6	15.5
10c	204.4	19.3
10d	176.3	54.4
10e	188.7	53.9
10f	187.5	81.86
10g	220.6	49.2
10h	196.0	69.0
10i	147.0 & 182.4	50.1

The variation of the inhibitory activity of several inhibitors against AChE and BChE can be explained by the slightly different molecular structures of the two enzymes. The different structures of the binding site and the amino acid sequence within the binding site[17] are certainly of great importance.

Also, the structural differences of compounds **10a–i** play an important role in the inhibitory activity. Methyl at position 12 (**10b**) and 13 (**10h**; see Figure 6 below) leads to improved biological activity compared to the nonsubstituted compound (**10a**). The introduction of two methyl groups (**10c**) leads to a slight loss of activity for AChE compared with the nonsubstituted compound (**10a**), but a slight improvement in the case of BChE. The introduction of one or two halogens (fluorine, chlorine) leads to only a slight activity drop compared with the nonsubstituted compound (**10a**). Interestingly, the introduction of only one halogen increases activity for AChE compared with two halogens but decreases activity for BChE in the case of chlorine.

2.4 | In vitro drug release

The aim of the testing was to describe the dissolution behavior of two synthesized sulfonamide derivatives that had the best inhibitory activity against AChE (**10b** and **10h**, see Table 3). A series of dissolution tests with these two substances incorporated into hydrophilic and lipophilic matrix has been performed at pH 1.2 and 4.5. The obtained dissolution profiles were quantitatively evaluated using appropriate mathematical models. The influence of pH and composition of tablets were studied. The dissolution behavior of the studied substances **10b** and **10h** is summarized in Figures 4 and 5. The similarity factor (f2) of the corresponding dissolution profiles was calculated (see Table 4). The dissolution profiles were fitted to the first-order kinetic model, Weibull model, and Korsmeyer–Peppas model. The summary of estimated parameters obtained from regression analysis of the dissolution profiles is shown in Tables 5–6, including the coefficient of determination (R^2).[10,11]

2.4.1 | Hydrophilic matrix tablets

For studied substances (**10b** and **10h**) similar dissolution profiles (fitted to Weibull model, see Figure 4) were achieved in both dissolution media (pH 1.2 and 4.5). A higher amount of drug release was achieved in a dissolution medium of pH 1.2 for both substances (**10b** and **10h**), with almost 90% of the substance **10b** released and almost 80% of the substance **10h** released after 24 h. In the case of a dissolution medium of pH 4.5, the release of substances was slightly slower, with nearly 60% of both substances (**10b** and **10h**) released after 24 h.

2.4.2 | Lipophilic matrix tablets

Release of studied active substances from the lipophilic matrix proceeded differently. For both substances (**10b** and **10h**) similar dissolution profiles (fitted to the Weibull model, see Figure 4) were achieved in both dissolution media (pH 1.2 and 4.5). Also, for both substances similar dissolution profiles (fitted to the first-order

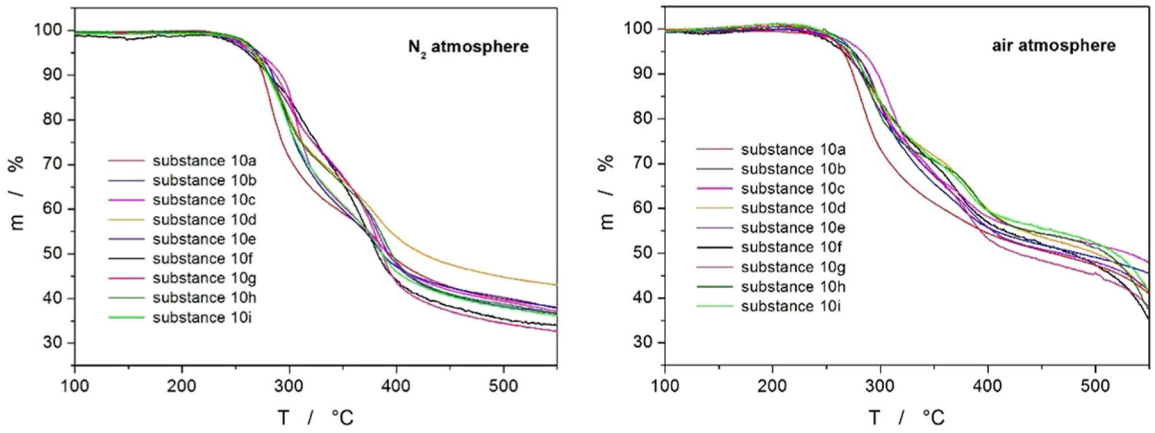

FIGURE 2 Thermogravimetric (TGA) curves obtained at 10°C·min^{-1} for substances **10a–i** either under N_2 or under air atmosphere.

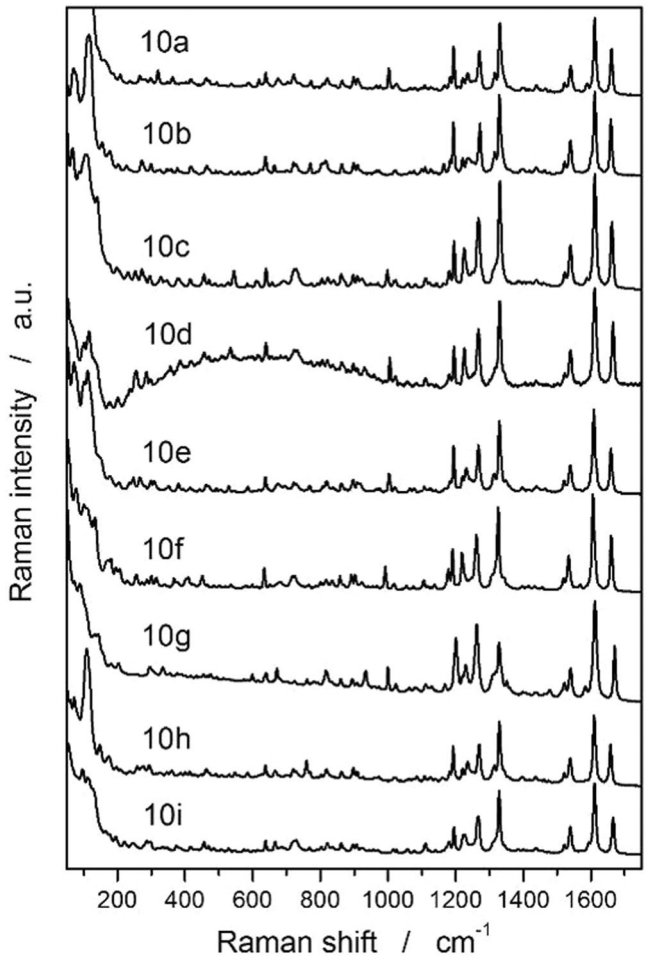

FIGURE 3 Raman spectra obtained for substances **10a–i**.

kinetic model) were achieved in the dissolution medium of pH 1.2. But overall, a relatively small amount of drug was released after 24 h. The drug release in the dissolution media of pH 1.2 and 4.5 is limited by the low solubility of the drug in these media. In the dissolution medium of pH 1.2, only about 12% (**10b**) and 15% (**10h**) were released after 24 h. The dissolution tests in the dissolution medium at pH 4.5 resulted in moderate improvement, with almost 18% of the active substance **10b** released and almost 32% of the substance **10h** released after 24 h.

So, higher amount of both substances (**10b** and **10h**) was released in the dissolution medium of pH 1.2 from the hydrophilic matrix.

In terms of structural correlation, the substances differ in one substituent (fluorine), thus differing in lipophilicity. Compound **10b** is slightly better released in a hydrophilic matrix than in a lipophilic matrix, which is consistent with its lower lipophilicity (LogP = 2.84) compared with compound **10h** (LogP = 3.14). In the lipophilic matrix,

TABLE 3 In vitro AChE and BChE inhibition of compounds 10a–i (IC_{50} (μM)) compared with that of standard rivastigmine (RIV).

	IC_{50} [μM]	
Comp.	**AChE**	**BChE**
10a	10.83 ± 0.36	104.98 ± 7.06
10b	7.95 ± 0.43	30.17 ± 1.17
10c	12.96 ± 0.02	94.55 ± 4.59
10d	17.13 ± 0.99	>500
10e	14.64 ± 0.09	138.31 ± 1.60
10f	14.90 ± 0.21	64.82 ± 0.01
10g	12.74 ± 0.51	146.67 ± 0.08
10h	7.35 ± 0.01	47.34 ± 0.71
10i	14.01 ± 0.04	28.88 ± 0.57
RIV	56.10 ± 1.41	38.40 ± 1.97

Note: Cholinesterase inhibition is expressed as the mean ± SD (n = 3 experiments).

Abbreviations: AChE, acetylcholinesterase; BChE, butyrylcholinesterase; RIV, rivastigmine.

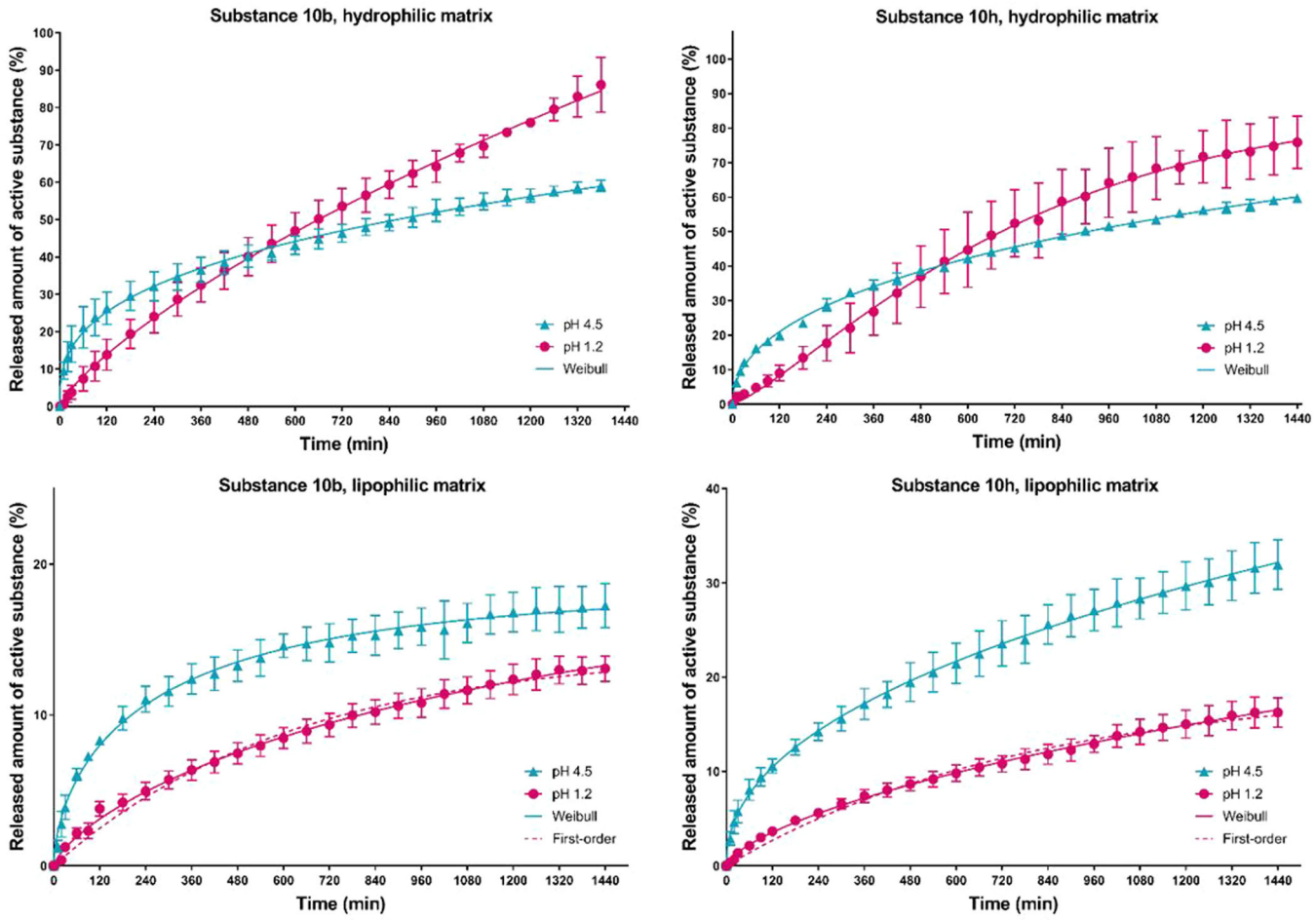

FIGURE 4 The dissolution profiles of selected substances **10b** and **10h** interlaced with the first-order and Weibull models. Error bars represent the standard deviation of the drug released ($n = 6$). Error bars for some points are smaller than the symbol.

the opposite is true. The predicted lipophilicities of these substances were calculated using SwissADME software.

2.5 | Regression analysis of the obtained dissolution profiles

Kinetic parameters were obtained from regression analysis (Tables 5–6) of the dissolution profiles, from which the active ingredient's release mechanism was deduced. In the case of substance **10b**, a hydrophilic matrix, the release took place in a dissolution medium of pH 1.2 by so-called anomalous transport, which is a combination of diffusion and other processes; it is a superposition of several transport mechanisms. In contrast, for the same substance in a dissolution medium of pH 4.5, the release was by "pure" diffusion. In the case of the same substance but a lipophilic matrix, the release in both media (pH 1.2 and 4.5) took place by "pure" diffusion. In the case of substance **10h**, a hydrophilic matrix, the release was based on swelling and relaxation of the carrier polymer chains in the dissolution medium of pH 1.2, and also by "pure" diffusion in the medium of pH 4.5. However, with the same active substance but a lipophilic matrix, the release took place by anomalous transport in a dissolution medium of pH 1.2 and again by "pure" diffusion in the case of a dissolution medium of pH 4.5.[10,11]

3 | CONCLUSION

A series of nine novel derivatives with sulfonamide and amide functional groups were prepared by multistep synthesis. Their successful preparation was confirmed using NMR spectrometry, elemental analysis, melting point analysis, and Raman spectroscopy. Good thermal stability and potential of these substances for the processing by means of hot-melt extrusion and 3D printing were verified via DSC and thermogravimetric (TGA) measurements. It has to be borne in mind that certain compounds exhibited complex melting behavior, which may indicate increased difficulty of their separation/isolation and a necessity for the consequent refining. The testing of biological activity on AD has shown that all nine derivatives are, under the given reaction conditions, more effective in inhibiting AChE than the standard RIV. In addition, two derivatives were found to be more potent in inhibiting BChE than the standard RIV. The

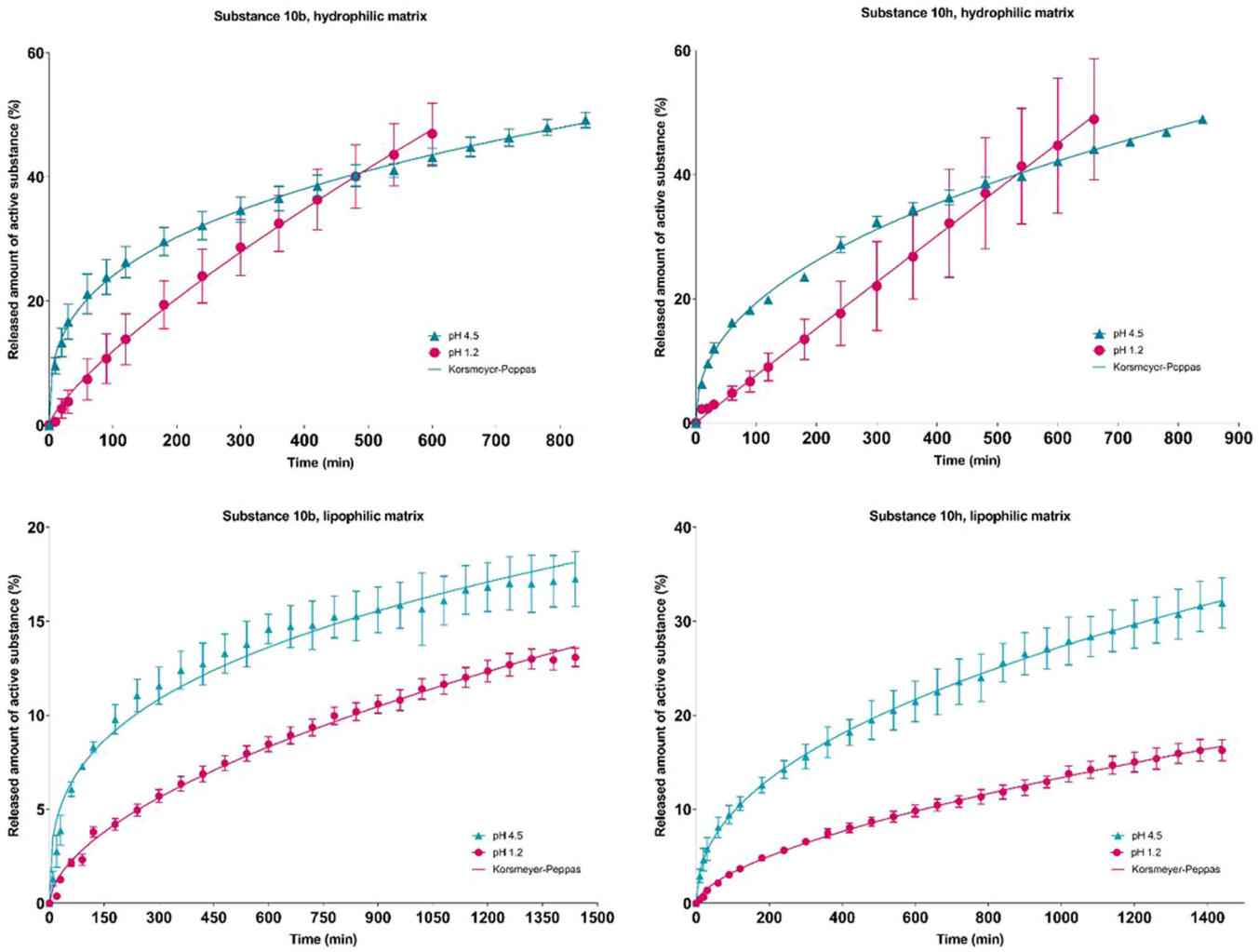

FIGURE 5 The dissolution profiles of selected substances **10b** and **10h** interlaced with the Korsmeyer–Peppas model. Error bars represent the standard deviation of the drug released ($n = 6$). Error bars for some points are smaller than the symbol.

TABLE 4 The computed similarity factors (f2).

	10b, hydrophilic matrix, pH 1.2	10b, hydrophilic matrix, pH 4.5	10b, lipophilic matrix, pH 1.2	10b, lipophilic matrix, pH 4.5
10h, hydrophilic matrix, pH 1.2	f2 = 74.32	x	x	x
10h, hydrophilic matrix, pH 4.5	x	f2 = 75.92	x	x
10h, lipophilic matrix, pH 1.2	x	x	f2 = 85.08	x
10h, lipophilic matrix, pH 4.5	x	x	x	f2 = 53.13

consequent dissolution testing of these two most promising sulfonamides (**10b** and **10h**) has revealed markedly better dissolution profiles in combination with the hydrophilic matrix (compared with the lipophilic formulation), reaching 75%–90% release in pH = 1.2, and 50%–60% release in pH = 4.5 (both during 24 h). The release took place mostly by "pure" diffusion or sometimes by anomalous transport. In conclusion, the favorable biological activity and dissolution behavior of the **10b** and **10h** compounds make them very promising drug candidates, worth further testing regarding the therapeutic and side effects, potential toxicity, and so on.

4 | EXPERIMENTAL

4.1 | Chemistry

4.1.1 | General

All reagents and solvents were purchased from commercial sources (Sigma Aldrich, Merck, Fluorochem, Lachema, Penta, LachNer, Acros Organics, Gattefossé SAS, JPS Pharma GMBH & CO). Commercial-grade reagents were used without further purification. The prepared

TABLE 5 Regression analysis of substance 10b interlaced with the first-order, Weibull, and the Korsmeyer–Peppas models.

Substance 10b		First-order: $M_t = M_\infty(1 - \exp(-k_1 t))$ $k_1 \pm SD$ [hour^{-1}]	R^2
pH 1.2	Hydrophilic matrix	0.048 ± 0.012	0.9862
pH 4.5		0.228 ± 0.06	0.8734
pH 1.2	Lipophilic matrix	0.096 ± 0.012	0.9714
pH 4.5		0.3 ± 0.042	0.9347

		Weibull: $M_t = M_\infty(1 - \exp(-k_w t^\beta))$ $k_w \pm SD$ [hour$^{-\beta}$]	β ± SD	R^2
pH 1.2	Hydrophilic matrix	0.048 ± 0.024	1.06 ± 0.07	0.9835
pH 4.5		2.118 ± 0.36	0.44 ± 0.03	0.9706
pH 1.2	Lipophilic matrix	0.282 ± 0.042	0.73 ± 0.06	0.9778
pH 4.5		1.842 ± 0.306	0.61 ± 0.04	0.9658

		Korsmeyer–Peppas: $\frac{M_t}{M_\infty} = k_{KP} t^n$ $n \pm SD$	R^2
pH 1.2	Hydrophilic matrix	0.77 ± 0.04	0.9699
pH 4.5		0.33 ± 0.01	0.9581
pH 1.2	Lipophilic matrix	0.57 ± 0.02	0.9742
pH 4.5		0.33 ± 0.01	0.9423

TABLE 6 Regression analysis of substance 10h interlaced with the first-order, Weibull, and the Korsmeyer–Peppas models.

Substance 10h		First-order: $M_t = M_\infty(1 - \exp(-k_1 t))$ $k_1 \pm SD$ [hour^{-1}]	R^2
pH 1.2	Hydrophilic matrix	0.048 ± 0.018	0.9589
pH 4.5		0.156 ± 0.024	0.9578
pH 1.2	Lipophilic matrix	0.078 ± 0.012	0.9737
pH 4.5		0.138 ± 0.024	0.9398

		Weibull: $M_t = M_\infty(1 - \exp(-k_w t^\beta))$ $k_w \pm SD$ [hour$^{-\beta}$]	β ± SD	R^2
pH 1.2	Hydrophilic matrix	0.018 ± 0.012	1.24 ± 0.13	0.9612
pH 4.5		0.774 ± 0.15	0.48 ± 0.02	0.9972
pH 1.2	Lipophilic matrix	0.156 ± 0.09	0.67 ± 0.07	0.9818
pH 4.5		0.756 ± 0.252	0.65 ± 0.05	0.9718

		Korsmeyer–Peppas: $\frac{M_t}{M_\infty} = k_{KP} t^n$ $n \pm SD$	R^2
pH 1.2	Hydrophilic matrix	0.99 ± 0.09	0.9307
pH 4.5		0.44 ± 0.01	0.9955
pH 1.2	Lipophilic matrix	0.61 ± 0.02	0.9815
pH 4.5		0.45 ± 0.01	0.9784

compounds (Figure 6) were characterized by nuclear magnetic resonance (NMR) spectroscopy (see the Supporting Information), elemental analysis, high-performance liquid chromatography (HPLC) analysis, melting point, Raman spectroscopy, and DSC analysis. Melting points were determined on a Melting Point B-540 apparatus (Büchi). The NMR spectra were measured in dimethyl sulfoxide-d_6 (dmso-d6) solutions or $CDCl_3$ solutions at ambient temperature on a Bruker AscendTM 500 spectrometer at frequencies ^{1}H (500.13 MHz), ^{13}C (125.77 MHz) and ^{19}F (202.49 MHz) and on a Bruker AscendTM 400 spectrometer at frequencies ^{1}H (400.13 MHz), ^{13}C (100.62 MHz), and ^{19}F (376.46 MHz). The proton chemical shifts, δ, are given in ppm, related to the residual solvent peaks (δ = 7.27 or 2.50 in $CDCl_3$ or DMSO-d_6, respectively). Carbon chemical shifts are referenced to the middle of the solvent's multiplet (δ = 77.0 or 39.5 in $CDCl_3$ or DMSO-d_6, respectively). The coupling constants (J) are reported in [Hz]. Elemental analysis (C, H, N, S) was performed on an automatic microanalyzer Flash 2000 Organic elemental analyzer. HPLC profiles (extracted ion chromatograms) together with MS profiles from negative mode, only substance **8** from positive mode, (see Supporting Information) were obtained using Agilent 1260 Infinity II PRIME liquid chromatographic system, equipped with a quaternary high-pressure pump, autosampler with integrated thermostated column compartment and diode-array UV detector (Agilent). Ionization of the compounds was carried out by electrospray and recording of positively and negatively charged ions was carried out in SCAN mode with a range of *m/z* 50–600. The fragmentation energy was set to 110 V. For substance **8**, a *m/z* range of 50–250 and a fragmentation energy of 60 V was used to increase the detection response. Thermal stability of the prepared compounds was determined using the differential scanning calorimeter DSC Q2000 (TA Instruments) equipped with an autosampler, RCS90 cooling accessory, and T-zero technology—the samples with masses 0.5–1 mg (accurately weighted to ± 0.01 mg) were hermetically sealed in aluminium (Al) pans and heated from 20°C to 230°C at 10°C·min^{-1}. In addition to the DSC analysis, TGA measurements were performed using the STA 449 F5 Jupiter instrument (Netzsch) equipped with a DSC/TG holder. The prepared compounds (similar sample masses as for the DSC measurements) were placed in open Al pans and heated up to 550°C at 10°C·min^{-1} under the constant 50 ml·min^{-1} flow of either air or N_2. Apart from the thermo-analytical

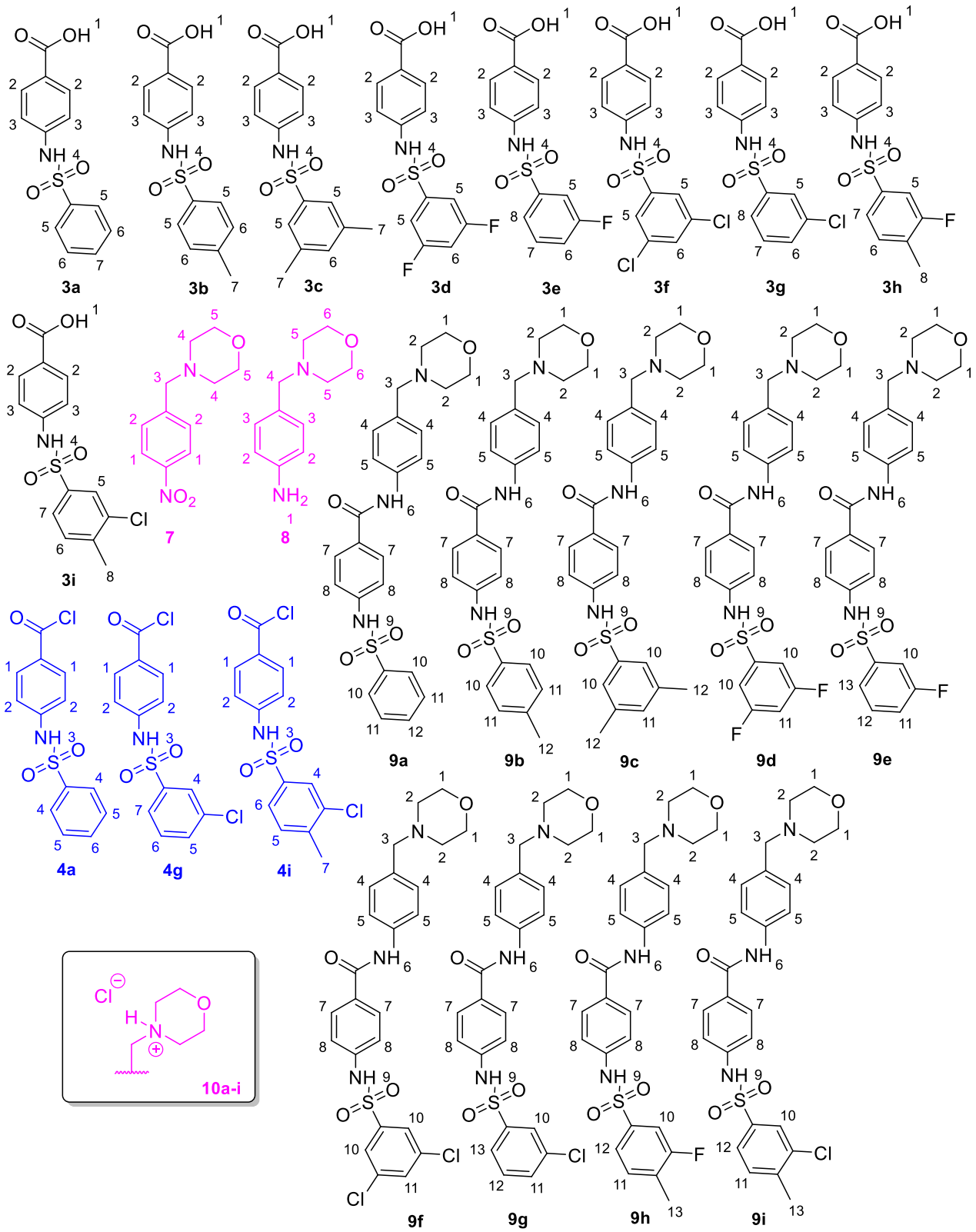

FIGURE 6 Numbered structures of the prepared compounds.

characterization, the synthesized compounds were also characterized by means of Raman spectroscopy, using the DXR2 Raman microscope (Thermo Fisher Scientific), equipped with the 785 nm excitation diode laser (30 mW, laser spot size 1.6–3.1 µm) and charged-couple device detector. The exact setup used for the measurements was: 10× objective & 25 µm collection slit, 20 mW laser power, 2 s collection per scan, 30 scans summed in one spectrum.

The InChI codes of the investigated compounds, together with some biological activity data, are provided as Supporting Information.

4.1.2 | General experimental procedure for the synthesis of the starting substances **3a–i**

Substances **3a–i** were prepared as follows: distilled water (60 mL) and 1 eq. of K_2CO_3 were added into a round bottom flask (100 mL), followed by the addition of 1 eq. of 4-aminobenzoic acid and finally 1 eq. of variously substituted benzenesulfonyl chloride. The reaction mixture was stirred at 90°C for 2–3 h. The reaction mixture is acidified by the addition of concentrated HCl (pH = 0–1). The product was recrystallized from a mixture of ethanol and water (70: 30). All of the starting materials were obtained with yields above 50%.

4-(Phenylsulfonamido)benzoic acid (**3a**): White solid; yield 84%; mp 207–209°C. ^{1}H NMR (500.13 MHz, dmso-d6): δ = 12.79 (1H, s, OH, H1); 10.87 (1H, s, NH, H4); 7.84 (4H, m, H2, H5); 7.61 (1H, t, ^3J = 7.2 Hz, H7); 7.56 (2H, t, ^3J = 7.2 Hz, H6); 7.23 (2H, d, ^3J = 8.8 Hz, H3). ^{13}C NMR (125.77 MHz, dmso-d6): δ = 166.9; 142.0; 139.3; 133.3; 130.9; 129.5; 126.8; 126.5; 125.7; 118.2. CHNS analysis: Calc. for $C_{13}H_{11}NO_4S$ (277.29): C, 56.31; H, 4.00; N, 5.05; S, 11.56. Found: C, 56.53; H, 4.01; N, 4.94; S, 11.50.

4-[(4-Methylphenyl)sulfonamido]benzoic acid (**3b**): White solid; yield 93%; mp 235–236°C. ^{1}H NMR (400.13 MHz, dmso-d6): δ = 12.73 (1H, s, OH, H1); 10.76 (1H, s, NH, H4); 7.80 (2H, d, ^3J = 8.8 Hz, H2); 7.71 (2H, d, ^3J = 8.3 Hz, H5); 7.35 (2H, d, ^3J = 8.3 Hz, H6); 7.20 (2H, d, ^3J = 8.8 Hz, H3); 2.31 (3H, s, CH_3, H7). ^{13}C NMR (100.62 MHz, dmso-d6): δ = 166.8; 143.7; 142.1; 136.4; 130.8; 129.9; 126.8; 125.5; 118.0; 21.0. CHNS analysis: Calc. for $C_{14}H_{13}NO_4S$ (291.32): C, 57.72; H, 4.50; N, 4.81; S, 11.01. Found: C, 57.32; H, 4.59; N, 4.52; S, 10.79.

4-[(3,5-Dimethylphenyl)sulfonamido]benzoic acid (**3c**): White solid; yield 68%; mp 240–242°C. ^{1}H NMR (500.13 MHz, dmso-d6): δ = 12.68 (1H, s, OH, H1); 10.88 (1H, s, NH, H4); 7.76 (2H, d, ^3J = 8.6 Hz, H2); 7.43 (2H, s, H5); 7.22 (1H, s, H6); 7.14 (2H, d, ^3J = 8.6 Hz, H3); 2.29 (6H, s, CH_3, H7). ^{13}C NMR (125.77 MHz, dmso-d6): δ = 167.2; 142.7; 140.0; 138.8; 134.3; 130.6; 126.2; 124.1; 118.1; 20.8. CHNS analysis: Calc. for $C_{15}H_{15}NO_4S$ (305.35): C, 59.00; H, 4.95; N, 4.59; S, 10.50. Found: C, 59.21; H, 4.93; N, 4.47; S, 10.43.

4-[(3,5-Difluorophenyl)sulfonamido]benzoic acid (**3d**): White-pinkish solid; yield 57%; mp 245–246°C. ^{1}H NMR (400.13 MHz, dmso-d6): δ = 12.82 (1H, s, OH, H1); 11.00 (1H, s, NH, H4); 7.85 (2H, d, ^3J = 8.6 Hz, H2); 7.63 (1H, dt, $^3J(^{19}F, ^1H)$ = 9.3 Hz, ^4J = 2.1 Hz, H6); 7.52 (2H, m, H5); 7.24 (2H, ^3J = 8.6 Hz, H3). ^{13}C NMR (100.62 MHz, dmso-d6): δ = 166.7; 163.5 (d, $^1J(^{19}F,^{13}C)$ = 252.3 Hz); 161.0 (d, $^1J(^{19}F,^{13}C)$ = 252.3 Hz); 142.5 (t, $^3J(^{19}F,^{13}C)$ = 8.3 Hz); 141.1; 130.9; 126.4; 118.8; 110.7 (d, $^2J(^{19}F,^{13}C)$ = 29.2 Hz); 109.3 (t, $^2J(^{19}F,^{13}C)$ = 26.0 Hz). ^{19}F NMR (376.46 MHz, dmso-d6): δ = −105.7. CHNS analysis: Calc. for $C_{13}H_9F_2NO_4S$ (313.27): C, 49.84; H, 2.90; N, 4.47; S, 10.23. Found: C, 49.96; H, 2.78; N, 4.43; S, 10.04.

4-[(3-Fluorophenyl)sulfonamido]benzoic acid (**3e**): White solid; yield 54%; mp 220–222°C. ^{1}H NMR (400.13 MHz, dmso-d6): δ = 12.79 (1H, s, OH, H1); 10.92 (1H, s, NH, H4); 7.81 (2H, d, ^3J = 8.7 Hz, H2); 7.64 (3H, m, H5, H7, H8); 7.51 (1H, dt, ^4J = 2.5 Hz, ^3J = 8.6 Hz, $^3J(^{19}F, ^1H)$ = 8.6 Hz, H6); 7.21 (2H, m, H3). ^{13}C NMR (100.62 MHz, dmso-d6): δ = 166.7; 161.7 (d, $^1J(^{19}F,^{13}C)$ = 249.3 Hz); 141.5; 141.2 (d, $^3J(^{19}F,^{13}C)$ = 6.8 Hz); 131.9 (d, $^3J(^{19}F,^{13}C)$ = 8.3 Hz); 130.8; 126.0; 123.0 (d, $^4J(^{19}F,^{13}C)$ = 3.0 Hz); 120.5 (d, $^2J(^{19}F,^{13}C)$ = 21.1 Hz); 118.5; 113.7 (d, $^2J(^{19}F,^{13}C)$ = 24.6 Hz). ^{19}F NMR (376.46 MHz, dmso-d6): δ = −110.0. CHNS analysis: Calc. for $C_{13}H_{10}FNO_4S$ (295.28): C, 52.88; H, 3.41; N, 4.74; S, 10.86. Found: C, 53.06; H, 3.36; N, 4.68; S, 11.24.

4-[(3,5-Dichlorophenyl)sulfonamido]benzoic acid (**3f**): White solid; yield 52%; mp 264-266°C. ^{1}H NMR (500.13 MHz, dmso-d_6): δ = 12.65 (1H, s, OH, H1); 10.98 (1H, s, NH, H4); 7.96 (1H, s, H6); 7.85 (2H, d, ^3J = 8.4 Hz, H2); 7.79 (2H, s, H5); 7.23 (2H, d, ^3J = 8.4 Hz, H3). ^{13}C NMR (125.77 MHz, dmso-d_6): δ = 166.6; 142.3; 141.0; 135.2; 133.0; 130.9; 126.5; 125.2; 118.9. CHNS analysis: Calc. for $C_{13}H_9Cl_2NO_4S$ (346.18): C, 45.10; H, 2.62; N, 4.05; S, 9.26. Found: C, 45.47; H, 2.59; N, 3.91; S, 9.45.

4-[(3-Chlorophenyl)sulfonamido]benzoic acid (**3 g**): White solid; yield 74%; mp 215–217°C. ^{1}H NMR (400.13 MHz, dmso-d_6): δ = 12.77 (1H, s, OH, H1); 10.92 (1H, s, NH, H4); 7.83 (2H, d, ^3J = 8.6 Hz, H2); 7.82 (1H, s, H5); 7.76 (1H, d, ^3J = 7.9 Hz, H6); 7.71 (1H, d, ^3J = 7.9 Hz, H8); 7.60 (1H, t, ^3J = 7.9 Hz, H7); 7.21 (2H, d, ^3J = 8.6 Hz, H3). ^{13}C NMR (100.62 MHz, dmso-d_6): δ = 166.7; 141.5; 141.1; 134.0; 133.3; 131.6; 130.9; 126.2; 126.1; 125.4; 118.6. CHNS analysis: Calc. for $C_{13}H_{10}ClNO_4S$ (311.74): C, 50.09; H, 3.23; N, 4.49; S, 10.28. Found: C, 50.31; H, 3.17; N, 4.34; S, 10.31.

4-[(3-Fluoro-4-methylphenyl)sulfonamido]benzoic acid (**3h**): White solid; yield 73%; mp 238–239°C. ^{1}H NMR (400.13 MHz, dmso-d6): δ = 12.75 (1H, s, OH, H1); 10.85 (1H, s, NH, H4); 7.82 (2H, d, ^{3}J = 8.6 Hz, H2); 7.55 (2H, m, H5, H7); 7.49 (1H, m, H6); 7.21 (2H, d, ^{3}J = 8.6 Hz, H3), 2.25 (3H, s, CH_3, H8). ^{13}C NMR (100.62 MHz, dmso-d_6): δ = 166.7; 160.0 (d, $^1J(^{19}F,^{13}C)$ = 248.4 Hz); 141.7; 138.4 (d, $^3J(^{19}F,^{13}C)$ = 6.7 Hz); 132.7 (d, $^3J(^{19}F,^{13}C)$ = 5.4 Hz); 130.8; 125.9; 122.7 (d, $^4J(^{19}F,^{13}C)$ = 3.4 Hz); 118.3; 113.3 (d, $^2J(^{19}F,^{13}C)$ = 25.5 Hz); 14.3 (d, $^3J(^{19}F,^{13}C)$ = 2.8 Hz). ^{19}F NMR (376.46 MHz, dmso-d_6): δ = −110.1. CHNS analysis: Calc. for $C_{14}H_{12}FNO_4S$ (309.31): C, 54.36; H, 3.91; N, 4.53; S, 10.36. Found: C, 54.13; H, 3.68; N, 4.30; S, 10.12.

4-[(3-Chloro-4-methylphenyl)sulfonamido]benzoic acid (**3i**): White solid; yield 65%; mp 236-238°C. ^{1}H NMR (400.13 MHz, dmso-d6): δ = 12.73 (1H, s, OH, H1); 10.87 (1H, s, NH, H4); 7.81 (3H, m, H2, H5); 7.66 (1H, t, ^{3}J = 7.9 Hz, H7); 7.55 (1H, d, ^{3}J = 7.9 Hz, H6); 7.21 (2H, d, ^{3}J = 8.5 Hz, H3); 2.35 (3H, CH_3, H8). ^{13}C NMR (100.62 MHz, dmso-d_6): δ = 166.7; 141.6; 138.4; 134.0; 132.2;

130.9; 126.7; 126.0; 125.8; 125.4; 118.4. CHNS analysis: Calc. for $C_{14}H_{12}ClNO_4S$ (325.76): C, 51.62; H, 3.71; N, 4.30; S, 9.84. Found: C, 51.59; H, 3.59; N, 4.07; S, 9.54.

4.1.3 | General experimental procedure for the synthesis of the starting substance **8**

Substance **8** was prepared by a two-step synthesis. In the first step, 4-nitrobenzylmorpholine (**7**) was prepared by reacting 4-nitro-1-chloromethylbenzene (20 g) with morpholine (22 g) in 200 mL of ethanol. After processing the reaction mixture, compound **7** was reduced with hydrazine hydrate to form 4-(morpholine-4-ylmethyl) aniline in the second reaction step. This reaction was carried out in methanol (161 mL), where an amount of $FeCl_3$ (0.48 g), charcoal (8.04 g), and 80% hydrazine hydrate (32.2 mL) were added to 4-nitrobenzylmorpholine (25.74 g), and the reaction mixture was maintained at 80°C for 3–4 h. After processing the reaction mixture, we obtained the desired substance **8** with a yield of 81%.

4-(4-Nitrobenzyl)morpholine (**7**): Yellow-orange solid; yield 79%; mp 75–77°C. ^{1}H NMR (400.13 MHz, dmso-d_6): δ = 8.18 (2H, d, ^3J = 8.7 Hz, H1); 7.59 (2H, d, ^3J = 8.7 Hz, H2); 3.59 (2H, m, H3); 3.57 (4H, m, H4); 2.36 (4H, m, H5). ^{13}C NMR (100.62 MHz, dmso-d_6): δ = 146.6; 146.4; 129.8; 123.4; 66.2; 61.4; 53.1. CHN analysis: Calc. for $C_{11}H_{14}N_2O_3$ (222.24): C, 59.45; H, 6.35; N, 12.61. Found: C, 59.32; H, 6.31; N, 12.69.

4-(Morpholine-4-ylmethyl)aniline (**8**): Yellowish solid; yield 81%; mp 98–99°C. ^{1}H NMR (400.13 MHz, dmso-d_6): δ = 6.91 (2H, d, ^3J = 8.2 Hz, H2); 6.51 (2H, d, ^3J = 8.2 Hz, H3); 4.95 (2H, s, NH_2); 3.53 (4H, m, H5); 3.25 (2H, m, H4); 2.28 (4H, m, H6). ^{13}C NMR (100.62 MHz, dmso-d_6): δ = 147.6; 129.9; 124.4; 113.6; 66.2; 62.4; 53.0. CHN analysis: Calc. for $C_{11}H_{16}N_2O$ (192.26): C, 68.72; H, 8.39; N, 14.57. Found: C, 68.57; H, 8.32; N, 14.66.

4.1.4 | General experimental procedure for the synthesis of the chlorides **4a–i**

The starting substances **3a–i** were converted to chlorides using $SOCl_2$. A total of 2 g of the substance, 60 mL of toluene, and 10 mL of $SOCl_2$ were put into a 100 mL round flask. The reaction mixture was heated at 90°C for 2 h. After processing the reaction mixture, recrystallization from the hexane: toluene mixture (1: 3) was carried out. Prepared substances **4a–i** were used in the next reaction step, but we have been able to characterize some of them by NMR.

4-(Phenylsulfonamido)benzoyl chloride (**4a**): ^{1}H NMR (400.13 MHz, $CDCl_3$): δ = 7.99 (2H, t, ^3J = 8.7 Hz, H1); 7.92 (2H, d, ^3J = 7.6 Hz, H4); 7.87 (1H, s, NH, H3); 7.61 (1H, t, ^3J = 7.6 Hz, H6); 7.51 (2H, t, ^3J = 7.6 Hz, H5); 7.21 (2H, d, ^3J = 8.7 Hz, H2). ^{13}C NMR (100.62 MHz, $CDCl_3$): δ = 167.2; 143.2; 138.4; 133.8; 133.3; 129.5; 128.6; 127.2; 118.2.

4-[(3-Chlorophenyl)sulfonamido]benzoyl chloride (**4g**): ^{1}H NMR (400.13 MHz, $CDCl_3$): δ = 8.02 (2H, d, ^3J = 8.8 Hz, H1); 7.91 (1H, t, ^4J = 1.8 Hz, H4); 7.79 (1H, s, NH, H3); 7.78 (1H, d, ^3J = 7.9 Hz, H5); 7.57 (1H, d, ^3J = 7.9 Hz, H7); 7.46 (1H, t, ^3J = 7.9 Hz, H6); 7.22 (2H, d, ^3J = 8.8 Hz, H2). ^{13}C NMR (100.62 MHz, $CDCl_3$): δ = 167.2; 142.6; 140.6; 135.7; 134.0; 133.3; 130.8; 129.0; 127.2; 125.3; 118.5.

4-[(3-Chloro-4-methylphenyl)sulfonamido]benzoyl chloride (**4i**): ^{1}H NMR (400.13 MHz, $CDCl_3$): δ = 8.00 (2H, d, ^3J = 8.8 Hz, H1); 7.89 (1H, d, ^4J = 1.9 Hz, H4); 7.84 (1H, s, NH, H3); 7.68 (1H, dd, ^3J = 8.0 Hz, ^4J = 1.9 Hz, H6); 7.35 (1H, d, ^3J = 8.0 Hz, H5); 7.21 (2H, d, ^3J = 8.8 Hz, H2); 2.41 (3H, CH_3, H7). ^{13}C NMR (100.62 MHz, $CDCl_3$): δ = 167.2; 143.1; 142.8; 137.1; 135.6; 133.3; 131.8; 128.8; 127.7; 125.3; 118.3; 20.4.

4.1.5 | General experimental procedure for the synthesis of the final sulfonamides and amides **9a–i**

Substances **4a–i** reacted with substance **8** to give the desired final compounds. 1 eq. of compounds **4a–i** and 50 mL of DCM were put in a 100 mL round bottom flask, and after dissolving, 1 eq. of substance **8** dissolved in 5 mL of DCM and 1.15 eq. of K_2CO_3 dissolved in 5 mL of distilled water were added. The reaction mixture was stirred for a day. After processing the reaction mixture, recrystallization was carried out from a methanol. Compounds **9a–i** were obtained in yields ranging from 31% to 75%.

N-[4-(Morpholine-methyl)phenyl]-4-(phenylsulfonamido) benzamide (**9a**): White solid; yield 71%; mp 180–182°C. ^{1}H NMR (500.13 MHz, dmso-d_6): δ = 10.76 (1H, s, NH, H9); 10.07 (1H, s, NH, H6); 7.86 (2H, d, ^3J = 7.6 Hz, H10); 7.80 (2H, d, ^3J = 8.5 Hz, H7); 7.65 (2H, d, ^3J = 8.3 Hz, H5); 7.63 (1H, t, ^3J = 7.6 Hz, H12); 7.57 (2H, t, ^3J = 7.6 Hz, H11); 7.24 (2H, d, ^3J = 8.3 Hz, H4); 7.19 (2H, d, ^3J = 8.5 Hz, H8); 3.56 (4H, m, H1); 3.40 (2H, s, H3); 2.33 (4H, m, H2). ^{13}C NMR (125.77 MHz, dmso-d_6): δ = 164.7; 141.2; 139.6; 138.1; 133.1; 132.8; 129.7; 129.4; 129.2; 129.0; 126.7; 120.1; 118.3; 66.2; 62.1; 53.1. CHNS analysis: Calc. for $C_{24}H_{25}N_3O_4S$ (451.54): C, 63.84; H, 5.58; N, 9.31; S, 7.10. Found: C, 63.87; H, 5.76; N, 9.67; S, 6.72.

4-[(4-Methylphenyl)sulfonamide]-*N*-[4-(morpholine-methyl) phenyl]benzamide (**9b**): White solid; yield 75%; mp 236–237°C. ^{1}H NMR (400.13 MHz, dmso-d_6): δ = 10.68 (1H, s, NH, H9); 10.07 (1H, s, NH, H6); 7.80 (2H, d, ^3J = 8.6 Hz, H7); 7.71 (2H, d, ^3J = 8.1 Hz, H10); 7.65 (2H, d, ^3J = 8.3 Hz, H5); 7.36 (2H, d, ^3J = 8.3 Hz, H4); 7.23 (2H, d, ^3J = 8.1 Hz, H11); 7.19 (2H, d, ^3J = 8.6 Hz, H8); 3.55 (4H, m, H1); 3.40 (2H, s, H3); 2.34 (3H, s, CH_3, H12); 2.33 (4H, m, H2). ^{13}C NMR (100.62 MHz, dmso-d_6): δ = 164.7; 143.6; 140.9; 138.0; 136.5; 132.8; 129.8; 129.2; 129.0; 126.8; 120.1; 118.2; 66.2; 62.0; 53.1; 21.0. CHNS analysis: Calc. for $C_{25}H_{27}N_3O_4S$ (465.57): C, 64.50; H, 5.85; N, 9.03; S, 6.89. Found: C, 64.52; H, 5.95; N, 8.92; S, 6.52.

4-[(3,5-Dimethylphenyl)sulfonamide]-*N*-[4-(morpholine-methyl) phenyl]benzamide (**9c**): White solid; yield 53%; mp 189–190°C. ^{1}H NMR (400.13 MHz, dmso-d_6): δ = 10.66 (1H, s, NH, H9); 10.07 (1H, s, NH, H6); 7.81 (2H, d, ^3J = 8.6 Hz, H7); 7.66 (2H, d, ^3J = 8.3 Hz, H5); 7.46 (2H, s, H10); 7.26 (1H, s, H11); 7.24 (2H, d, ^3J = 8.3 Hz, H4); 7.20 (2H, d, ^3J = 8.6 Hz, H8); 3.56 (4H, m, H1); 3.41 (2H, s, H3); 2.33

(4H, m, H2); 2.31 (6H, s, C$\underline{H}_3$, H12). ^{13}C NMR (100.62 MHz, dmso-d$_6$): δ = 164.7; 141.0; 139.4; 138.9; 138.1; 134.5; 132.8; 129.7; 129.2; 129.0; 124.1; 120.0; 118.0; 66.1; 62.0; 53.1; 20.7. CHNS analysis: Calc. for $C_{26}H_{29}N_3O_4S$ (479.60): C, 65.11; H, 6.10; N, 8.76; S, 6.68. Found: C, 65.08; H, 5.97; N, 8.52; S, 6.35.

4-[(3,5-Difluorophenyl)sulfonamide]-*N*-[4-(morpholine-methyl) phenyl]benzamide (**9d**): White solid; yield 57%; mp 210–212°C. ^{1}H NMR (400.13 MHz, dmso-d$_6$): δ = 10.35 (1H, s, N$\underline{H}$, H9); 10.12 (1H, s, N$\underline{H}$, H6); 7.83 (2H, d, ^3J = 9.4 Hz, H7); 7.66 (2H, d, ^3J = 8.2 Hz, H5); 7.61 (1H, t, ^3J(^{19}F, ^{1}H) = 8.9 Hz, H11); 7.52 (2H, m, H10); 7.23 (4H, m, H4, H8); 3.50 (4H, m, H1); 3.42 (2H, s, H3); 2.34 (4H, m, H2). ^{13}C NMR (100.62 MHz, dmso-d$_6$): δ = 164.8; 162.3 (d, ^1J(^{19}F,^{13}C) = 252.1 Hz); 162.1 (d, ^1J(^{19}F,^{13}C) = 252.1 Hz); 143.0 (t, ^3J(^{19}F,^{13}C) = 8.3 Hz); 140.7; 138.1; 132.7; 130.3; 129.3; 129.2; 120.2; 119.1; 110.6 (d, ^2J (^{19}F,^{13}C) = 28.1 Hz); 109.1 (t, ^2J(^{19}F,^{13}C) = 25.5 Hz); 66.2; 62.0; 53.1. ^{19}F NMR (376.46 MHz, dmso-d$_6$): δ = −105.9. CHNS analysis: Calc. for $C_{24}H_{23}F_2N_3O_4S$ (487.52): C, 59.13; H, 4.76; N, 8.62; S, 6.58. Found: C, 59.09; H, 4.81; N, 8.59; S, 6.28.

4-[(3-Fluorophenyl)sulfonamide]-*N*-[4-(morpholine-methyl) phenyl]benzamide (**9e**): White solid; yield 49%; mp 171–173°C. ^{1}H NMR (400.13 MHz, dmso-d$_6$): δ = 10.77 (1H, s, N$\underline{H}$, H9); 10.10 (1H, s, N$\underline{H}$, H6); 7.83 (2H, d, ^3J = 9.4 Hz, H7); 7.64 (5H, m, H5, H10, H12, H13); 7.51(1H, dt, ^4J = 2.5 Hz, ^3J = 8.7 Hz, ^3J(^{19}F, ^{1}H) = 8.7 Hz, H11); 7.23 (4H, m, H4, H8); 3.55 (4H, m, H1); 3.40 (2H, s, H3); 2.33 (4H, m, H2). ^{13}C NMR (100.62 MHz, dmso-d$_6$): δ = 164.7; 161.7 (d, ^1J(^{19}F,^{13}C) = 249.8 Hz); 141.4 (d, ^3J(^{19}F,^{13}C) = 7.2 Hz); 140.6; 138.0; 132.8; 131.9 (d, ^3J(^{19}F,^{13}C) = 7.3 Hz); 130.2; 129.2; 129.1; 120.2; 123.0 (d, ^4J(^{19}F,^{13}C) = 3.1 Hz); 120.3 (d, ^2J(^{19}F,^{13}C) = 21.4 Hz); 120.1; 118.7; 113.7 (d, ^2J(^{19}F,^{13}C) = 23.9 Hz); 66.1; 62.0; 53.1. ^{19}F NMR (376.46 MHz, dmso-d$_6$): δ = −110.1. CHNS analysis: Calc. for $C_{24}H_{24}FN_3O_4S$ (469.53): C, 61.39; H, 5.15; N, 8.95; S, 6.83. Found: C, 61.56; H, 5.22; N, 8.95; S, 6.51.

4-[(3,5-Dichlorophenyl)sulfonamide]-*N*-[4-(morpholine-methyl) phenyl]benzamide (**9f**): White solid; yield 31%; mp 229–231°C. ^{1}H NMR (500.13 MHz, dmso-d$_6$): δ = 10.66 (1H, s, N$\underline{H}$, H9); 10.07 (1H, s, N$\underline{H}$, H6); 7.94 (1H, s, H11); 7.81 (2H, d, ^3J = 8.6 Hz, H7); 7.63 (2H, s, H10); 7.65 (2H, d, ^3J = 8.3 Hz, H5); 7.24 (2H, d, ^3J = 8.3 Hz, H4); 7.18 (2H, d, ^3J = 8.6 Hz, H8); 3.54 (4H, m, H1); 3.41 (2H, s, H3); 2.33 (4H, m, H2). ^{13}C NMR (125.77 MHz, dmso-d$_6$): δ = 164.7; 142.3; 141.0; 139.4; 138.9; 138.1; 135.2; 133.0; 130.9; 129.2; 126.5; 125.2; 118.9; 66.1; 62.0; 53.1. CHNS analysis: Calc. for $C_{24}H_{23}Cl_2N_3O_4S$ (520.43): C, 55.39; H, 4.45; N, 8.07; S, 6.16. Found: C, 55.24; H, 4.38; N, 7.96; S, 6.21.

4-[(3-Chlorophenyl)sulfonamide]-*N*-[4-(morpholine-methyl) phenyl]benzamide (**9g**): White solid; yield 51%; mp 212–214°C. ^{1}H NMR (400.13 MHz, dmso-d$_6$): δ = 10.92 (1H, s, N$\underline{H}$, H9); 10.10 (1H, s, N$\underline{H}$, H6); 7.83 (1H, s, H10); 7.82 (2H, d, ^3J = 8.2 Hz, H7); 7.77 (1H, d, ^3J = 7.9 Hz, H11); 7.72 (1H, d, ^3J = 7.9 Hz, H13); 7.66 (2H, d, ^3J = 8.2 Hz, H5); 7.61 (1H, t, ^3J = 7.9 Hz, H12); 7.23 (4H, m, H4, H8); 3.55 (4H, m, H1); 3.40 (2H, s, H3); 2.33 (4H, m, H2). ^{13}C NMR (100.62 MHz, dmso-d$_6$): δ = 164.7; 141.3; 140.5; 138.1; 134.0; 133.2; 132.8; 131.5; 130.3; 129.2; 129.1; 126.2; 125.5; 120.1; 118.7; 66.2; 62.0; 53.1. CHNS analysis: Calc. for $C_{24}H_{24}ClN_3O_4S$ (485.98): C, 59.32; H, 4.98; N, 8.65; S, 6.60. Found: C, 59.36; H, 4.98; N, 8.69; S, 6.34.

4-[(3-Fluoro-4-methylphenyl)sulfonamide]-*N*-[4-(morpholine-methyl)phenyl]benzamide (**9h**): White solid; yield 58%; mp 208–209°C. ^{1}H NMR (400.13 MHz, dmso-d$_6$): δ = 10.79 (1H, s, N$\underline{H}$, H9); 10.09 (1H, s, N$\underline{H}$, H6); 7.87 (2H, d, ^3J = 8.7 Hz, H7); 7.67 (2H, d, ^3J = 8.5 Hz, H5); 7.55 (2H, m, H10, H12); 7.50 (1H, m, H11); 7.25 (2H, d, ^3J = 8.5 Hz, H4); 7.22 (2H, d, ^3J = 8.7 Hz, H8); 3.56 (4H, m, H1); 3.40 (2H, s, H3); 2.33 (4H, m, H2); 2.26 (3H, C$\underline{H}_3$, H13). ^{13}C NMR (100.62 MHz, dmso-d$_6$): δ = 164.7; 160.0 (d, ^1J(^{19}F,^{13}C) = 246.2 Hz); 140.8; 138.7 (d, ^3J(^{19}F,^{13}C) = 6.9 Hz); 132.8; 132.7 (d, ^3J(^{19}F,^{13}C) = 4.7 Hz); 130.6; 130.4; 130.0; 129.2; 129.0; 122.7 (d, ^4J(^{19}F,^{13}C) = 3.4 Hz); 120.1; 118.5; 113.3 (d, ^2J(^{19}F,^{13}C) = 25.4 Hz); 66.2; 62.0; 53.1; 14.3 (d, ^3J(^{19}F,^{13}C) = 2.8 Hz). ^{19}F NMR (376.46 MHz, dmso-d$_6$): δ = −110.1. CHNS analysis: Calc. for $C_{25}H_{26}FN_3O_4S$ (483.56): C, 62.10; H, 5.42; N, 8.69; S, 6.63. Found: C, 62.16; H, 5.28; N, 8.71; S, 6.30.

4-[(3-Chloro-4-methylphenyl)sulfonamide]-*N*-[4-(morpholine-methyl)phenyl]benzamide (**9i**): White solid; yield 67%, mp 193–195°C. ^{1}H NMR (400.13 MHz, dmso-d$_6$): δ = 10.90 (1H, s, N$\underline{H}$, H9); 10.11 (1H, s, N$\underline{H}$, H6); 7.84 (3H, m, H7, H10); 7.77 (1H, d, ^3J = 7.8 Hz, H11); 7.73 (2H, d, ^3J = 7.8 Hz, H5); 7.61 (1H, t, ^3J = 7.8 Hz, H12); 7.23 (4H, m, H4, H8); 3.56 (4H, m, H1); 3.42 (2H, s, H3); 2.34 (4H, m, H2); 2.34 (3H, C$\underline{H}_3$, H13). ^{13}C NMR (100.62 MHz, dmso-d$_6$): δ = 164.7; 141.5; 140.5; 138.5; 138.0; 134.0; 132.8; 132.2; 131.5; 130.2; 129.2; 129.1; 126.7; 125.4; 120.0; 118.6; 66.1; 62.0; 53.1; 19.7. CHNS analysis: Calc. for $C_{25}H_{26}ClN_3O_4S$ (500.01): C, 60.05; H, 5.24; N, 8.40; S, 6.41. Found: C, 59.95; H, 5.19; N, 8.35; S, 6.27.

4.1.6 | General experimental procedure for the converting of the substances **9a–i** into hydrochlorides **10a–i**

The final substances **9a–i** were converted into hydrochlorides using HCl. 1 eq. of the substances **9a–i** were dissolved in 20 mL of methanol and 1.15 eq. of conc. HCl was added. The reaction was stirred for 6 h, after which the resulting products (compounds **10a–i**) were filtered off.

4-(Phenylsulfonamide)-*N*-[4-(morpholine-methyl)phenyl] benzamide hydrochloride (**10a**): White solid; yield 98%, mp 211–213°C. ^{1}H NMR (400.13 MHz, dmso-d$_6$): δ = 11.21 (1H, s, $\underline{H}$Cl); 10.86 (1H, s, N$\underline{H}$, H9); 10.32 (1H, s, N$\underline{H}$, H6); 7.86 (4H, m, H5, H10); 7.81 (2H, d, ^3J = 8.5 Hz, H7); 7.64 (1H, t, ^3J = 7.6 Hz, H12); 7.57 (4H, m, H4, H11); 7.19 (2H, d, ^3J = 8.7 Hz, H8); 4.27 (2H, s, H3); 3.91 (2H, d, ^2J = 11.4 Hz, H1); 3.79 (2H, t, ^2J = 11.4 Hz, H1); 3.20 (2H, d, ^2J = 12.4 Hz, H2); 3.05 (2H, t, ^2J = 12.4 Hz, H2). ^{13}C NMR (100.62 MHz, dmso-d$_6$): δ = 165.0; 141.0; 140.4; 139.3; 133.2; 132.0; 130.0; 129.5; 129.2; 126.7; 124.0; 120.1; 118.3; 63.1; 58.6; 50.5. CHNS analysis: Calc. for $C_{24}H_{26}ClN_3O_4S$ (488.00): C, 59.07; H, 5.37; N, 8.61; S, 6.57. Found: C, 58.79; H, 5.53; N, 8.36; S, 6.28.

4-[(4-Methylphenyl)sulfonamide]-*N*-[4-(morpholine-methyl) phenyl]benzamide hydrochloride (**10b**): White solid; yield 91%, mp 196–198°C. ^{1}H NMR (400.13 MHz, dmso-d_6): δ = 11.04 (1H, s, *H*Cl); 10.76 (1H, s, N*H*, H9); 10.30 (1H, s, N*H*, H6); 7.82 (4H, m, H7, H10); 7.72 (2H, d, ^{3}J = 7.6 Hz, H5); 7.54 (2H, d, ^{3}J = 7.6 Hz, H4); 7.36 (2H, d, ^{3}J = 7.9 Hz, H11); 7.22 (2H, d, ^{3}J = 7.6 Hz, H8); 4.26 (2H, s, H3); 3.92 (2H, d, ^{2}J = 11.9 Hz, H1); 3.78 (2H, t, ^{2}J = 11.9 Hz, H1); 3.20 (2H, d, ^{2}J = 12.2 Hz, H2); 3.06 (2H, t, ^{2}J = 12.2 Hz, H2); 2.32 (3H, s, C*H*$_3$, H12). ^{13}C NMR (100.62 MHz, dmso-d_6): δ = 165.1; 143.7; 141.1; 140.4; 136.5; 132.0; 129.9; 129.5; 129.1; 126.8; 123.9; 120.1; 118.2; 63.1; 58.7; 50.5; 21.0. CHNS analysis: Calc. for $C_{25}H_{28}ClN_3O_4S$ (502.03): C, 59.81; H, 5.62; N, 8.37; S, 6.39. Found: C, 59.64; H, 5.83; N, 8.08; S, 6.02.

4-[(3,5-Dimethylphenyl)sulfonamide]-*N*-[4-(morpholine-methyl) phenyl]benzamide hydrochloride (**10c**): White solid; yield 99%, mp 204–206°C. ^{1}H NMR (400.13 MHz, dmso-d_6): δ = 11.04 (1H, s, *H*Cl); 10.77 (1H, s, N*H*, H9); 10.31 (1H, s, N*H*, H6); 7.85 (2H, d, ^{3}J = 8.6 Hz, H7); 7.81 (2H, d, ^{3}J = 8.3 Hz, H5); 7.55 (2H, d, ^{3}J = 8.3 Hz, H4); 7.47 (2H, s, H10); 7.26 (1H, s, H11); 7.23 (2H, d, ^{3}J = 8.6 Hz, H8); 4.26 (2H, s, H3); 3.91 (2H, d, ^{2}J = 11.5 Hz, H1); 3.79 (2H, t, ^{2}J = 11.5 Hz, H1); 3.19 (2H, d, ^{2}J = 12.1 Hz, H2); 3.06 (2H, t, ^{2}J = 12.1 Hz, H2); 2.30 (6H, s, C*H*$_3$, H12). ^{13}C NMR (100.62 MHz, dmso-d_6): δ = 164.7; 141.0; 139.4; 138.9; 138.1; 134.5; 132.8; 129.7; 129.2; 124.1; 123.9; 120.0; 118.0; 66.1; 62.0; 53.1; 20.7. CHNS analysis: Calc. for $C_{26}H_{30}ClN_3O_4S$ (516.05): C, 60.51; H, 5.86; N, 8.14; S, 6.21. Found: C, 60.25; H, 5.61; N, 7.86; S, 5.89.

4-[(3,5-Difluorophenyl)sulfonamide]-*N*-[4-(morpholine-methyl) phenyl]benzamide hydrochloride (**10d**): White solid; yield 70%, mp 185–187°C. ^{1}H NMR (400.13 MHz, dmso-d_6): δ = 11.05 (1H, s, *H*Cl); 10.94 (1H, s, N*H*, H9); 10.34 (1H, s, N*H*, H6); 7.87 (2H, d, ^{3}J = 8.8 Hz, H7); 7.81 (2H, d, ^{3}J = 8.5 Hz, H5); 7.65 (1H, dt, $^{3}J(^{19}F,^{1}H)$ = 9.2 Hz, ^{4}J =;2.2 Hz, H11); 7.55 (4H, m, H4, H10); 7.28 (4H, d, ^{3}J = 8.8 Hz, H8); 4.27 (2H, s, H3); 3.93 (2H, d, ^{2}J = 11.3 Hz, H1); 3.76 (2H, t, ^{2}J = 11.3 Hz, H1); 3.20 (2H, d, ^{2}J = 12.1 Hz, H2); 3.06 (2H, t, ^{2}J = 12.1 Hz, H2). ^{13}C NMR (100.62 MHz, dmso-d_6): δ = 165.0; 162.2 (d, $^{1}J(^{19}F,^{13}C)$ = 252.9 Hz); 162.1 (d, $^{1}J(^{19}F,^{13}C)$ = 252.9 Hz); 142.5 (t, $^{3}J(^{19}F,^{13}C)$ = 8.3 Hz); 140.3; 140.1; 131.9; 130.4; 129.3; 129.2; 120.1; 119.0; 110.6 (d, $^{2}J(^{19}F,^{13}C)$ = 28.6 Hz); 109.2 (t, $^{2}J(^{19}F,^{13}C)$ = 25.4 Hz); 63.1; 58.7; 50.5. ^{19}F NMR (376.46 MHz, dmso-d_6): δ = −105.9. CHNS analysis: Calc. for $C_{24}H_{24}ClF_2N_3O_4S$ (523.98): C, 55.01; H, 4.62; N, 8.02; S, 6.12. Found: C, 54.84; H, 4.76; N, 7.71; S, 5.86.

4-[(3-Fluorophenyl)sulfonamide]-*N*-[4-(morpholine-methyl) phenyl]benzamide hydrochloride (**10e**): White solid; yield 93%, mp 188–190°C. ^{1}H NMR (400.13 MHz, dmso-d_6): 10.94 (1H, s, *H*Cl); 10.82 (1H, s, N*H*, H9); 10.32 (1H, s, N*H*, H6); 7.85 (2H, d, ^{3}J = 8.6 Hz, H7); 7.80 (2H, d, ^{3}J = 8.5 Hz, H5); 7.65 (3H, m, H10, H12, H13); 7.52 (3H, m, H4, H11); 7.25 (2H, d, ^{3}J = 8.6 Hz, H8); 4.26 (2H, s, H3); 3.92 (2H, d, ^{2}J = 11.2 Hz, H1); 3.74 (2H, t, ^{2}J = 11.2 Hz, H1); 3.20 (2H, d, ^{2}J = 12.1 Hz, H2); 3.06 (2H, t, ^{2}J = 12.1 Hz, H2). ^{13}C NMR (100.62 MHz, dmso-d_6): δ = 165.1; 161.7 (d, $^{1}J(^{19}F,^{13}C)$ = 248.9 Hz); 141.3 (d, $^{3}J(^{19}F,^{13}C)$ = 6.7 Hz); 140.6; 140.4; 132.1 (d, $^{3}J(^{19}F,^{13}C)$ = 7.5 Hz); 132.0; 130.1; 129.3; 123.1 (d, $^{4}J(^{19}F,^{13}C)$ = 2.9 Hz); 120.5 (d, $^{2}J(^{19}F,^{13}C)$ = 20.9 Hz); 120.2; 118.7; 113.8 (d, $^{2}J(^{19}F,^{13}C)$ = 24.7 Hz); 63.2; 58.8; 50.6. ^{19}F NMR (376.46 MHz, dmso-d_6): δ = −110.1. CHNS analysis: Calc. for $C_{24}H_{25}ClFN_3O_4S$ (505.99): C, 56.97; H, 4.98; N, 8.30; S, 6.34. Found: C, 56.57; H, 5.14; N, 7.94; S, 6.19.

4-[(3,5-Dichlorophenyl)sulfonamide]-*N*-[4-(morpholine-methyl) phenyl]benzamide hydrochloride (**10f**): White solid; yield 79%, mp 187–189°C. ^{1}H NMR (400.13 MHz, dmso-d_6): δ = 11.08 (1H, s, *H*Cl); 10.80 (1H, s, N*H*, H9); 10.33 (1H, s, N*H*, H6); 7.86 (2H, d, ^{3}J = 8.8 Hz, H7); 7.80 (2H, d, ^{3}J = 8.5 Hz, H5); 7.57 (2H, d, ^{3}J = 8.3 Hz, H4); 7.50 (2H, s, H10); 7.28 (1H, s, H11); 7.21 (2H, d, ^{3}J = 8.6 Hz, H8); 4.26 (2H, s, H3); 3.91 (2H, d, ^{2}J = 11.5 Hz, H1); 3.75 (2H, t, ^{2}J = 11.5 Hz, H1); 3.21 (2H, d, ^{2}J = 12.1 Hz, H2); 3.07 (2H, t, ^{2}J = 12.1 Hz, H2). ^{13}C NMR (100.62 MHz, dmso-d_6): δ = 164.9; 141.6; 140.0; 139.2; 138.5; 134.8; 132.8; 129.5; 129.3; 124.5; 123.9; 120.8; 118.1; 63.1; 54.5; 50.4. CHNS analysis: Calc. for $C_{24}H_{24}Cl_3N_3O_4S$ (556.88): C, 51.76; H, 4.34; N, 7.55; S, 5.76. Found: C, 51.62; H, 4.30; N, 7.49; S, 5.81.

4-[(3-Chlorophenyl)sulfonamide]-*N*-[4-(morpholine-methyl) phenyl]benzamide hydrochloride (**10g**): White solid; yield 88%, mp 220–223°C. ^{1}H NMR (400.13 MHz, dmso-d_6): δ = 11.07 (1H, s, *H*Cl); 10.96 (1H, s, N*H*, H9); 10.33 (1H, s, N*H*, H6); 7.87 (5H, m, H5, H7, H10); 7.79 (1H, d, ^{3}J = 8.3 Hz, H13); 7.74 (1H, d, ^{3}J = 8.3 Hz, H11); 7.63 (1H, t, ^{3}J = 8.3 Hz, H12); 7.55 (2H, d, ^{3}J = 7.9 Hz, H4); 7.26 (2H, d, ^{3}J = 7.9 Hz, H8); 4.27 (2H, s, H3); 3.93 (2H, d, ^{2}J = 12.1 Hz, H1); 3.78 (2H, t, ^{2}J = 12.1 Hz, H1); 3.20 (2H, d, ^{2}J = 12.1 Hz, H2); 3.05 (2H, t, ^{2}J =;12.1 Hz, H2). ^{13}C NMR (100.62 MHz, dmso-d_6): δ = 165.0; 141.1; 140.5; 140.3; 134.0; 133.3; 131.9; 131.6; 130.1; 129.2; 126.2; 125.5; 123.9; 120.1; 118.7; 63.1; 58.6; 50.5. CHNS analysis: Calc. for $C_{24}H_{25}Cl_2N_3O_4S$ (522.44): C, 55.18; H, 4.82; N, 8.04; S, 6.14. Found: C, 55.33; H, 4.59; N, 7.70; S, 5.81.

4-[(3-Fluoro-4-methylphenyl)sulfonamide]-*N*-[4-(morpholine-methyl)phenyl]benzamide hydrochloride (**10h**): White solid; yield 74%, mp 203–205°C. ^{1}H NMR (400.13 MHz, dmso-d_6): δ = 11.03 (1H, s, *H*Cl); 10.88 (1H, s, N*H*, H9); 10.32 (1H, s, N*H*, H6); 7.86 (2H, d, ^{3}J = 8.7 Hz, H7); 7.81 (2H, d, ^{3}J = 8.5 Hz, H5); 7.55 (5H, m, H4, H10, H11, H12); 7.24 (2H, d, ^{3}J = 8.7 Hz, H8); 4.27 (2H, s, H3); 3.93 (2H, d, ^{2}J = 12.0 Hz, H1); 3.77 (2H, t, ^{2}J = 12.0 Hz, H1); 3.19 (2H, d, ^{2}J = 12.1 Hz, H2); 3.06 (2H, t, ^{2}J = 12.1 Hz, H2); 2.26 (3H, C*H*$_3$, H13). ^{13}C NMR (100.62 MHz, dmso-d_6): δ = 165.0; 160.0 (d, $^{1}J(^{19}F,^{13}C)$ = 247.1 Hz); 140.7; 140.3; 138.5 (d, $^{3}J(^{19}F,^{13}C)$ = 7.0 Hz); 132.8 (d, $^{3}J(^{19}F,^{13}C)$ = 4.9 Hz); 130.7; 130.6; 129.9; 129.2; 122.8 (d, $^{4}J(^{19}F,^{13}C)$ = 3.2 Hz); 120.1; 118.5; 113.4 (d, $^{2}J(^{19}F,^{13}C)$ = 25.6 Hz); 63.1; 58.7; 50.5; 14.3 (d, $^{3}J(^{19}F,^{13}C)$ = 3.0 Hz). ^{19}F NMR (376.46 MHz, dmso-d_6): δ = −110.1. CHNS analysis: Calc. for $C_{25}H_{27}ClFN_3O_4S$ (520.02): C, 57.74; H, 5.23; N, 8.08; S, 6.17. Found: C, 57.46; H, 5.36; N, 7.86; S, 5.86.

4-[(3-Chloro-4-methylphenyl)sulfonamide]-*N*-[4-(morpholine-methyl)phenyl]benzamide hydrochloride (**10i**): White solid; yield 82%, mp 182-185°C. ^{1}H NMR (400.13 MHz, dmso-d_6): δ = 11.00 (1H, s, *H*Cl); 10.87 (1H, s, N*H*, H9); 10.32 (1H, s, N*H*, H6); 7.86 (2H, d, ^{3}J = 8.8 Hz, H7); 7.82 (1H, s, H10); 7.80 (2H, d, ^{3}J = 8.5 Hz, H4); 7.69 (1H, d, ^{3}J = 8.2 Hz, H12); 7.56 (1H, d, ^{3}J = 8.2 Hz, H11); 7.54 (2H, d, ^{3}J = 8.5 Hz, H8); 7.25 (2H, d, ^{3}J = 8.5 Hz, H5); 4.27 (2H, s, H3); 3.93 (2H, d, ^{2}J = 11.6 Hz, H1); 3.76 (2H, t, ^{2}J = 11.6 Hz, H1); 3.19 (2H, d,

^{2}J = 11.6 Hz, H2); 3.06 (2H, t, ^{2}J = 11.6 Hz, H2); 2.36 (3H, CH_3, H13). ^{13}C NMR (100.62 MHz, dmso-d_6): δ = 164.9; 141.5; 140.5; 140.3; 138.5; 134.0; 132.2; 131.9; 130.0; 129.2; 126.7; 125.4; 120.1; 118.6; 63.1; 58.7; 50.5; 19.7. CHNS analysis: Calc. for $C_{25}H_{27}Cl_2N_3O_4S$ (536.47): C, 55.97; H, 5.07; N, 7.83; S, 5.98. Found: C, 55.58; H, 4.90; N, 7.52; S, 5.70.

4.2 | AChE and BChE inhibition studies

The ability of the synthesized derivatives to inhibit eeAChE (AChE from electric eel, *Electrophorus electricus*) and eqBChE (BChE from equine serum) was determined in vitro using Ellman's method.[14] Ellman's method is widely used for measuring cholinesterase activity and the efficiency of cholinesterase inhibitors. The principle of this simple method is the determination of the SH and –S–S– groups. The activity of the cholinesterase is measured indirectly by quantifying the concentration of 2-nitro-5-sulfanylbenzoic acid ion formed in the reaction between 5,5′-dithiobis-2-nitrobenzoic acid (DTNB) and thiocholine.

The ability of the studied substances to inhibit eeAChE and eqBChE was determined at 25°C in the presence of phosphate-buffered saline (PBS, 0.1 M, pH 7.4) in a glass cuvette with a 1 cm optical path. The enzyme activity in the total reaction mixture (2 mL) was 0.2 U/mL; the amount of acetylthiocholine (ATCh) or butyrylthiocholine (BTCh) was 0.08 mL (1×10^{-3} M); and the amount of DTNB was 0.4 mL (5×10^{-4} M) for all reactions. The inhibitory activity of the studied derivatives was evaluated based on the ratio v_0/v_i (v_0 is the rate of ATCh or BTCh hydrolysis in the absence of the inhibitor, v_i is the rate of ATCh or BTCh hydrolysis in the presence of the inhibitor). The IC_{50} values were obtained from the dependence v_0/v_i on the concentration of the tested substances (inhibitors).

The determination of v_0 was done as follows: PBS, DTNB, and ATCh/BTCh were added into the cuvette. The enzymatic reaction was started by adding the enzyme. The dependence of absorbance (λ = 412 nm) on time was observed for 70 s (the reference solution contained PBS, DTNB, ATCh, or BTCh), and then the reaction rate was calculated ($v = \Delta A/\Delta t$). The measurement was performed at least in triplicate, and the average v_0 was determined.

Subsequently, v_i was determined as follows: DTNB, ATCh/BTCh, a chosen volume of the suitably diluted inhibitor (the concentration of which was chosen so that the resulting v_0/v_i ratio was higher than 1), and a certain volume of PBS (to achieve the total volume of the reaction mixture 2 mL after adding the enzyme) were placed into the cuvette. The enzymatic reaction was started again by adding the enzyme. The dependence of absorbance (λ = 412 nm) on time was observed for 70 s (the reference solution was the same as for the reaction in the absence of the inhibitor), and then the reaction rate (v_i) was calculated. Four different concentrations of the inhibitor were used, and each measurement was performed at least in duplicate but mostly triplicate. Finally, the dependence v_0/v_i on the concentration of the inhibitor was determined, and IC_{50} was calculated from the obtained equation of the regression curve for $y = 2$ (based on the definition of IC_{50}).[14]

The IC_{50} value depends to some extent on the reaction conditions and therefore on the method used. Different values of IC_{50} for RIV are given in the literature.[5,18,19] In our study, both the standard and the samples were measured under the same reaction conditions and by using the same method. It is proven, that all nine derivatives are, under the given reaction conditions, more effective in inhibiting AChE than the standard RIV.

4.3 | Preparation of lipophilic and hydrophilic matrix tablets by direct compression method

The composition of studied lipophilic and hydrophilic matrix tablets is described in Table 7. The tablets were prepared by the direct compression method at a constant compression force of 8 kN. Compounds **10b** and **10h** were used as the active pharmaceutical ingredients (API). The API and excipients were blended in a mixer (RETSCH MM200, Retsch), and the prepared mixtures were directly compressed on a 13 mm flat punch set using a manual single-punch tablet press (H-62-TRYSTOM s.r.o., Olomouc). The tablets were of cylindrical shape without facets with a diameter of 13 mm and a weight of 500 ± 5 mg. For one dissolution test, six tablets with the active ingredient and one tablet without the active ingredient were compressed as the blank sample. In the blank samples, the amount of the API was replaced with the microcrystalline cellulose (Prosolv® SMCC 90).

4.4 | In vitro drug-release studies

Drug-release tests were carried out with a dissolution apparatus (Sotax AT 7 Smart) using the paddle method. All dissolution tests were performed according to the *European Pharmacopeia*[9] in a paddle arrangement. Two different dissolution media prepared according to the *Ph. Eur.* were used: (1) an acidic medium at pH 1.2 (HCl with an adjustment of ionic strength using NaCl); (2) a duodenum medium at pH 4.5. One dissolution test lasted 24 h with a stirring rate of 100 rpm. Such a long period of time for the dissolution test was chosen because of the unknown behavior of the new sulfonamides. The bath temperature was maintained at 37 ± 0.5°C throughout the test. During the dissolution tests at predetermined time intervals, 3 mL aliquots of the dissolution medium were automatically withdrawn and filtered. Each experiment

TABLE 7 The composition of the matrix tablets studied in %.

Hydrophilic matrix	Lipophilic matrix	Mass (%)
Prosolv® SMCC 90	Prosolv® SMCC 90	39
API	API	20
Methocel™ K4M	Compritol® 888 ATO	40
Magnesium stearate	Magnesium stearate	1

was performed with six tablets and one blank sample. In all dissolution tests, the released amount of the drug was determined using UV–Vis spectrometry, and the dissolution profiles obtained were evaluated using suitable kinetic models.[9]

4.5 | Determination of the drug-release amount using UV–Vis spectrometry

An HP Agilent 8453 spectrophotometer (Agilent Technologies) was used to determine drug (**10b** and **10h**) concentration in the dissolution samples. The absorbance values of the samples withdrawn at the predetermined times were measured against the corresponding blank sample using the fixed-wavelength method. A wavelength of 276 nm for pH 1.2 and 4.5, together with three-point background correction, was applied. The used wavelengths corresponded to the absorption maximum of the drugs (**10b** and **10h**). The validity of the Lambert–Beer law was verified in the expected range of the drug concentrations. The calibration-curve method was used to transform the absorbance values into the concentrations and percentages. These percentages were plotted against time to obtain the dissolution profile of the drug.

4.6 | Nonlinear regression analysis of dissolution profiles

To quantitatively evaluate the released amount of the drug (**10b** and **10h**) from the studied matrix tablets, the obtained dissolution profiles were fitted to the Weibull (1) and the first-order kinetic (2) models expressed by the following equations:

$$M_t = M_\infty(1 - \exp(-k_w t^\beta)), \quad (1)$$

$$M_t = M_\infty(1 - \exp(-k_1 t)). \quad (2)$$

In Equation (1), M_t is the amount of the drug released in time t, M_∞ is the maximum releasable amount of the drug in infinite time, and k_w is a constant of the Weibull model with unit $time^{-\beta}$. Parameter β characterizes the shape of the exponential curve. In Equation (2), M_t is the amount of the drug released in time t, M_∞ is the maximum releasable amount of the drug in infinite time, and k_1 is a first-order rate constant with unit $time^{-1}$.[10,11]

The obtained dissolution profiles were also fitted to the Korsmeyer–Peppas model (3), which applies only if the amount of drug released does not exceed 60% and it's expressed by the following equation:

$$\frac{M_t}{M_\infty} = k_{KP} t^n. \quad (3)$$

From this model, we can infer the mechanism of drug release. In Equation (3), M_t is the amount of the drug released in time t, M_∞ is the maximum releasable amount of the drug in infinite time, and k_{KP} is a constant with unit $time^{-n}$, where parameter n characterizes the transport mechanism, the mechanism of release, of the drug from the dosage form. GraphPad Prism 9.3.1 (GraphPad Software) was employed for the nonlinear regression analysis.[10,11]

ACKNOWLEDGMENTS

This work was supported by the Internal Grant Agency of the University of Pardubice under the SGS project. Open access publishing facilitated by Univerzita Pardubice, as part of the Wiley - CzechELib agreement.

CONFLICTS OF INTEREST STATEMENT

The authors declare no conflicts of interest.

DATA AVAILABILITY STATEMENT

The data that support the findings of this study are available from the corresponding author upon reasonable request.

ORCID

Marie Nevyhoštěná http://orcid.org/0009-0006-9004-5430

REFERENCES

[1] *World Health Organization: Neurological disorders affect millions globally: WHO report*. (online) Brussels: © 2023 WHO, 2007. (cit. March 16, 2023) https://www.who.int/news/item/27-02-2007-neurological-disorders-affect-millions-globally-who-report

[2] M. Zvěřová, *Clin. Biochem.* **2019**, *72*, 3. https://doi.org/10.1016/j.clinbiochem.2019.04.015

[3] T. M. Ghazal, S. Abbas, S. Munir, M. A. Khan, M. Ahmad, G. F. Issa, S. B. Zahra, M. A. Khan, M. K. Hasan. *Comput. Mater. Cont.* **2022**, *70*(3), 5005. https://doi.org/10.32604/cmc.2022.020866

[4] G. F. Makhaeva, S. V. Lushchekina, N. V. Kovaleva, T. Yu. Astakhova, N. P. Boltneva, E. V. Rudakova, O. G. Serebryakova, A. N. Proshin, I. V. Serkov, T. P. Trofimova, V. A. Tafeenko, E. V. Radchenko, V. A. Palyulin, V. P. Fisenko, J. Korábečný, O. Soukup, R. J. Richardson, *Bioorg. Chem.* **2021**, *112*, 104974. https://doi.org/10.1016/j.bioorg.2021.104974

[5] G. Marucci, M. Buccioni, D. D. Ben, C. Lambertucci, R. Volpini, F. Amenta, *Neuropharmacology* **2021**, *190*(108352), 108352. https://doi.org/10.1016/j.neuropharm.2020.108352

[6] J. Korábečný, E. Nepovimová, T. Cikánková, K. Špilovská, L. Vašková, E. Mezeiová, K. Kuča, J. Hroudová, *Neuroscience* **2018**, *370*, 191. https://doi.org/10.1016/j.neuroscience.2017.06.034

[7] S. Akocak, M. Boga, N. Lolak, M. Tuneg, R. K. K. Sanku, *J. Turkish Chem. Soc. Sect. A Chem.* **2019**, *6*(1), 63. https://doi.org/10.18596/jotcsa.516444

[8] A. Nordberg, C. Ballard, R. Bullock, T. Darreh-Shori, M. Somogyi, *Prim. Care Companion CNS Disord.* **2013**, *15*(2). https://doi.org/10.4088/PCC.12r01412

[9] European Pharmacopoeia 11th Edition, Strasbourg, France: European Directorate for the Quality of Medicines & Healthcare, **2022**.

[10] J. Muselík, A. Komersová, V. Lochař, K. Kubová, In: *Chemické listy*, Česká společnost chemická, Praha **2019**, 113(5), pp. 328

[11] J. Muselík, A. Komersová, K. Kubová, K. Matzick, B. Skalická, *Pharmaceutics* **2021**, *13*(10), 1703. https://doi.org/10.3390/pharmaceutics13101703

[12] P. J. Das, B. Sarmah, *Asian J. Chem.* **2015**, *27*(1), 189. https://doi.org/10.14233/ajchem.2015.16853

[13] Z. Šimková, Bc. SYNTÉZA BIOLOGICKY AKTIVNÍCH SULFONAMIDOVÝCH DERIVÁTŮ (MORFOLIN-4-YLMETHYL)ANILINU. Pardubice, **2020**. Diplomová práce. Univerzita Pardubice, Fakulta chemicko-technologická. Vedoucí práce Doc. Ing. Vladimír Pejchal, Ph.D. https://hdl.handle.net/10195/76203

[14] G. Šinko, M. Čalić, A. Bosak, Z. Kovarik, *Anal. Biochem.* **2007**, *370*(2), 223. https://doi.org/10.1016/j.ab.2007.07.023

[15] *DrugBank*. The Canadian Institutes of Health Research: Educe Design & Innovation Inc. (online), **2006**. (cit. April 14, 2022) https://go.drugbank.com/

[16] D. Voet, J. G. Voet. *Biochemie*. Praha: Victoria Publishing, **2005**. ISBN 80-856-0544-9.

[17] B. Brus, U. Košak, S. Turk, A. Pišlar, N. Coquelle, J. Kos, J. Stojan, J. P. Colletier, S. Gobec, *J. Med. Chem.* **2014**, *57*(19), 8167. https://doi.org/10.1021/jm501195e

[18] H. Ogura, T. Kosasa, Y. Kuriya, Y. Yamanishi, *Methods Find. Exp. Clin. Pharmacol.* **2000**, *22*(8), 609. https://doi.org/10.1358/mf.2000.22.8.701373

[19] J. Wu, M. Pistolozzi, S. Liu, W. Tan, *Bioorg. Med. Chem.* **2020**, *28*(5), 115324. https://doi.org/10.1016/j.bmc.2020.115324

SUPPORTING INFORMATION

Additional supporting information can be found online in the Supporting Information section at the end of this article.

How to cite this article: M. Nevyhoštěná, A. Komersová, V. Pejchal, Š. Štěpánková, P. Česla, K. Matzick, J. Macháčková, R. Svoboda, *Arch. Pharm.* **2024**;*357*:e2400191. https://doi.org/10.1002/ardp.202400191